FNAL E781 H-note 712, December 15, 1994

First Test of E781 Photon Calorimeter Readout

V. Steiner, M.A. Moinester, A. Ocherashvili, S. Gerzon and S. Kananov
Tel Aviv Univ., 69978 Ramat Aviv, Israel

P. Cooper, J. Engelfried
Fermilab, Batavia, Illinois, USA

D. Mao, J. Russ
Carnegie-Mellon Univ., Pittsburg, Pennsylvania, USA

E. de Oliveira
CBPF, Rio de Janeiro, Brasil

S.B. Nurushev
IHEP, 142284 Protvino, Moskow, Russia

M. Svoiski
Nuclear Physics Institute, St. Petersburg, Russia

Abstract

We describe first readout tests carried out at FNAL during August 1994 of an E781 lead-glass detector. We used a single lead-glass channel of the Photon 4 calorimeter and the basic elements of the anticipated complete readout system. We injected light pulses into the lead-glass counter using a very simple light distribution system. A green LED coupled to a bundle of optical fibers was installed in the calorimeter, and was fired from upstream via a cable, approximatelly 66 m in length. A bundle of approximately 40 optical fibers were used to inject 100 nsec light pulses into the front side of the lead-glass block. Signals from the FEU-84-3 phototube, viewing the opposite end of the block, were sent back, upstream and integrated in the prototype LRS 1881 charge sensitive ADC, located in a FASTBUS crate. The ADC readout was performed using a simple C-code running via the VxWorks operating system, in a Fastbus Smart Crate Controller (FSCC) computer located in the same crate. The digitized data was transferred to the Challenge FN781A host computer and analysed. We present typical spectra of the signal and the pedestal for different ADC inputs, as well as their stability and dispersion over monitoring periods of 1-3 days. There are 64 ADC inputs for each ECL module. Measurements of the calorimeter temperature, carried out in parallel via a sensor located inside Photon 4, are shown for comparison. In addition, we present sytematic measurements of the lead-glass detector response to various levels of light, for a large range of high voltages of the FEU-84-3 phototube, carried out with a similar setup at Tel-Aviv Univ. Some useful information is given for getting started with FSCC, VxWorks and Fastbus.

1 Goal

The goal of the present work is to perform and describe first readout tests of a photon calorimeter using the complete readout system forseen, thereby to get a first glance at the ADC pedestal and signal stability for a single lead-glass channel under off-beam conditions.

The four E781 photon calorimeters are designed to cover a large energy range extending to $\approx$ 20, 50 and 300 GeV for Photon 1, 2 and 3/4 respectively. With the 8196-channel and 400 pC range of the 1881M charge sensitive ADC [1], this corresponds to a charge resolution of 48.8 fC/channel and an energy resolution of 2.4, 6.1 and 36.6 MeV/channel respectively. Our need is to preserve this fine energy resolution, during long periods of data taking in the E781 PC4 environment. This sets very severe demands on the stability and noise level of the ADC channels.

2 Experimental setup

The basic experimental setup used during the measurements is shown in Fig. 1. It was assembled in the PC4 vault where the E781 detectors are being installed now. Among them are Photon 3 and 4, nearly fully equipped and located presently at $\approx$ 60 m downstream from the target. This is retracted by $\sim$ 10 m from its foreseen position. We choose to use Photon 4 mainly because of its more convenient location. We used one cable from a bundle of 33 coaxial cables, with a length of 66 m, linking it from the Photon 4 location to an electronics rack located a few meters downstream from the target.

2.1 Photon 4 calorimeter

The Photon 4 calorimeter consists of an $x \times y$ array of 21×16 lead-glass detectors, with a central 2×4 hole for the beam, i.e. a total of 328 counters. The detectors are closely stacked and alligned vertically by steel bands. Each detector consists of a $38.2 \times 38.2 \times 450$ mm^3 block of SF5 lead-glass, coupled by optical grease to a FEU-84-3 phototube.

The high voltage supply is provided by a LeCroy 1440 system. The phototubes are arranged in groups of 8 units which have similar gain and therefore may receive the same voltage. The voltage of the different groups is tuned such as the equalize the gain of all the phototubes of the calorimeter. However the voltages of the last 4 dynodes of all the phototubes are exactly the same, and are provided by an external 4-module Booster Power Supply (BPS). The BPS ensures a voltage stability better than 0.1% and is essential to maintain the phototube gains at high counting rates [5]. In the present tests the booster supplies were not used, because rates were low. Instead, Zener diodes developped the same voltages for each of the 4 dynodes that would have come from the booster supplies.

At the front plane, the calorimeter is provided for each lead-glass channel with two holes. A small ($\approx$ 1 mm diameter) central hole allows inserting a single optical fiber, and fixing it by a rubber washer and a nut. A larger hole located at the lower-right corner

Dynode	Voltage (V)	Current (mA)
9	-70	20
10	-102	30
11	-158	~ 40
12	-230	~ 50

Table 1: The voltages and currents provided by the BPS on the four last dynodes of the FEU-84-3 phototube

(≈ 10 mm diameter) allows coupling a larger light source. The front plane is light shielded from outside by a removable cover. In the space between the front plane and the cover, a light distribution system, supplying calibration light to the detectors, was installed (see Section 2.3 for details).

The calorimeter is enclosed in a metal housing which may be moved in the (x,y) directions perpendicular to the beam, such as to position each lead-glass block in the beam for callibration. This housing shields the lead-glass detectors from outside light, magnetic fields and may be flushed with a neutral gas in order to avoid phototube heating.

2.2 FEU-84-3 phototube

The FEU-84-3 phototube [4] provides a charge signal proportional to the light burst inside the lead-glass block. It has a 12-dynode venetian blind structure, a sensitive diameter of 25 mm covered by a trialkaline (Sb-K-Na-Cs) photocathode of type S-200, with a photosensitivity of $> 10^{-4}$ A/lm and maximal quantum efficiency at 410 nm. The tube has an outer diameter of 34 mm and is enclosed in a μ-metal tube providing magnetic shielding [5].

The phototube base has a special construction in that the voltages and currents for the last dynodes $9-12$ are provided externally by the BPS, as shown in Table 1. The rest of the dynode voltages are set using a conventional base.

During the present work, in which we used only one phototube, we did not connect the BPS. Instead, we used a simple equivalent circuit, essentialy an ensemble of daisy chained Zener diodes, which provided (together with the base) the correct dynode voltages [6]. In Fig. 1, we refer to it as the "Magic box". The absolute high voltage for the Magic box was provided by a Fluke power supply.

2.3 Light distribution system

The role of the light distribution system is to inject light pulses of constant amplitude into each lead-glass detector. Normally, the phototube response should also be constant. Any detected change signals a change of the calibration constant, and is used to recalculate it [7]. As described in Section 2.1, the light distribution system was mounted on the Photon 4 front plane.

The system (see Fig. 1) consists of a light box optically coupled to a bundle of optical fibers, running to the lead-glass detectors. In order to provide sufficient light, about 40 fibers were bundled together and fed to a particular lead-glass block (ref. number 22115) of Photon 4, which we choose for testing in this work.

2.3.1 Light box

The light box serves to couple the light source into the fibers. It consists of a cylindrical plastic box, with a length of $\approx$ 10 cm and a diameter of $\approx$ 4 cm. It contains an LED, which illuminates a bundle of optical fibers via a diffusor located in the middle of the box.

2.3.2 Light source

The light source (see the detail in Fig. 1) consists of a green LED [2], whose cathode is connected to ground via a 50 Ω resistor. We fired it by short 30-100 nsec square pulses provided by a pulser, with a maximal +5 V amplitude, applied at the anode. The measured pulse height attenuation of the pulser signal over the cable length of 66 m was only 5%, while its square shape was only slightly modified by the cable capacitance. We expect the same attenuation of the pulse height of the phototube signal. Its time integral however, i.e. the charge, should be unaffected by the cable length.

2.3.3 Diffusor

The diffusor has the role to equalize the amount of light coupled to the fibers by reflecting the LED light in many directions. It is made of a thin paper membrane.

2.3.4 Fiber bundle

The fiber bundle consists of 576 plastic fibers attached and glued together forming a rigid structure with a diameter of $\approx$ 3 cm. The fiber heads were cut and polished to provide good light transmission. Each fiber has a diameter of $\approx$ 1 mm and a variable length of $\approx 20 - 80$ cm, adjusted such as to reach all Photon 4 channels.

2.3.5 Light variation in the bundle

The variation of the light intensity coupled into the optical fibers over the area of the bundle is an important parameter, since it determines the range of equivalent energy for monitoring in the lead-glass detectors coupled to the bundle. Ideally, all lead-glass detectors in a calorimeter should be monitored at the same energy. Therefore, it is desirable to minimize this illumination variation, such that supplementary corrections by adjusting of the phototube voltages is not necessary.

The variation of illumination over the area of the fiber bundle was studied using *four* different light distribution systems (with the same construction and dimensions as described above) and the same LED as the light source. The LED was fired by a +5 V square signal, 500 ns in length, delivered by a pulser. The illumination variation in each bundle was determined by connecting each fiber in the bundle to a FEU-84-3 phototube, and measuring on a scope the pulse height of the phototube signal. The phototube voltage, delivered by a Fluke power supply, was kept constant at −1300 V. Measurements in which the fibers were exposed to the neon light in the room were hindered by noise. This noise disappeared when the fibers were covered. It was therefore due to variations of the light intensity in the room, and coupled into the fibers. This noise was removed by using the simple filter circuit, shown in Fig. 2. This solution allowed to carry out the measurements with uncovered fibers, since it eliminated the influence of both the DC level and the low frequency (60 Hz) light variations in the room.

In Fig. 3 we show the fiber-to-fiber variation of light intensity in Bundle number 4, which was used for ADC readout in the present work. The measured rms width of the light intensity in its 576 fibers is as large as 23%. The attenuation introduced by the light box (essentially by the paper diffusor) is not know. This important quantity should be measured since we need to minimize light losses.

In Fig. 4 (a)-(d) we compare the fiber-to-fiber light intensity variation in the case of the four fiber bundles (the Bundle 4 is shown in (d)). The rms variation of illumination over the fiber bundle area is nearly the same and quite large, namely 31% (a), 24% (b), 25% (c), and 23% (d). A much better performance, namely an illumination uniformization, of $\approx 3\%$, and a very small light attenuation of only a few percent was achieved in Tel Aviv Univ. tests by using a prismatic mixing rod made of plexiglass, instead of the paper diffusor [7].

2.4 Electronics

The basic electronics used in this work is shown in Fig. 1. A pulser delivered a positive square signal of variable amplitude, width and rate, as well as a NIM trigger signal. The amplitude and the trigger signals were sent downstream on adjacent cables. The amplitude signal fired the LED while the trigger was routed back upstream. The lead-glass signal followed it after the short transit time through the phototube. The trigger (after proper delay) was fed to a 821 discriminator generating a 100 nsec gate and then fed to a 4616 NIM-ECL convertor, providing the ADC gate. The phototube signal was directly fed to one of 64 inputs of the prototype 1881 charge sensitive ADC located in a FASTBUS crate. We used the prototype ADC since the nominal 1881M ADC was not operational.

2.5 Data acquisition

In the same crate with the ADC, a Fastbus Smart Crate Controller (FSCC) computer was installed and linked to Ethernet. General information on our software is given in the Appendix. The readout of the ADC was carried out by means of a C-code running in the FSCC via the VxWorks operating system. A sample list of this code is given in the Appendix.

Typical events consisted of signals and/or pedestals of various ADC inputs taken with a 100 nsec gate and at rate of 1 kHz. Normally, only one single channel had a lead-glass signal, while the rest contained pedestals. In order to monitor for the same channel both signal and pedestal at essentially the same time, a second 100 ns gate, delayed by 500 msec with respect to the first was generated. The digitized data was transfered to the FN781A (Challenge) host computer, stored on disk and later analysed using CERN software.

In order to investigate the possible influence of the PC4 vault temperature on the signal or pedestal stability, a second C-code was written and run in parallel with the ADC readout. This code read perodically the Photon 4 temperature by means of a sensor mounted close to the LED, via the EPICURE monitoring system of FNAL.

3 Results

3.1 Lead-glass signal

The amount of light coupled into the lead-glass block by a single optical fiber was insufficient. In order to produced a clear signal, above the noise level of ± 1 mV, the phototube voltage had to be pushed as high as -1800 V. Instead, we bundled about 40 fibers together, which increased the amount of light and gave a clear ≈ 25 mV signal at a phototube voltage of -1500 V.

Typical signal shapes are shown schematically in Fig. 5. The LED was fired by a short 30 nsec square pulse, at a frequency of 1 kHz, and a variable amplitude between ≈ 1 V (the threshold for light emission) and 5 V (the maximum delivered by the pulser). We notice the rather long tail of the signal, due to the slow LED response, which could not be completely integrated in the 100 nsec gate of the experiment. We performed measurements also with gates as large as 500 nsec, the maximum gate accepted by the ADC (see Section 3.3 for details).

3.2 Lead-glass spectrum

The first lead-glass spectrum was obtained using a qVt 3001 unit, instead of the ADC. This was a fast procedure, very useful to find the best LED pulsing conditions, the required light level in the lead-glass block, and the phototube high voltage needed in order to obtain a good signal in the $0 - 400$ pC range of the ADC.

In Fig. 6 we show typical spectra of the lead-glass signal (a) and pedestal (b) using the setup shown in Fig. 1. This is the integral spectrum of a ≈ 14 hour monitoring run shown in Fig. 9. Using the ADC calibration of 50 fC/channel, the net signal (after pedestal subtraction) corresponds to 14 pC. The signal dispersion (after quadratically subtracting the pedestal noise) is equal to 0.53 pC or 3.8% of the signal, consistent with a typical short time-scale LED performance. We also note that the pedestal noise is rather large. In absolute terms, the net signal dispersion (10.7 channels) is equal to the pedestal noise (10.3 channels). We discuss the pedestal noise in more detail in Section 3.5.

3.3 Lead-glass response

We tried to measure the response of the lead-glass detector to various levels of light and high voltages, in order to find the region of linearity. This could not be properly done in the present setup, because the LED light output was too long (exceeding the 100 nsec. gate of the E781 experiment) and also not proportional to the input voltage pulse height. For reference purpose only, we carried out the measurements by stetching the ADC gate to the maximum of 500 nsec., in order to integrate most of the signal. The extent of this non-linearity may be seen in Fig. 7. The correct measurement should use a fast laser pulse, or a faster LED fired by a short current pulse. The light can then be precisely attenuated by calibrated filters. In Section 4, we show measurement results obtained using filters.

3.4 Lead-glass stability

The stability of the lead-glass signal and pedestal was studied by taking periodical measurements of those spectra over periods of $1-3$ days, for different ADC channels, under stable conditions. We increased the statistics such that the centroid accuracy was much better compared with the measured variations. For each spectrum, we computed the average channel position and the rms width and we recorded the sampling time.

In Fig. 8 we show the variation of the lead- glass spectrum centroid (a) and rms width (b) over ≈ 58 hours of continuous monitoring. There were 116 measurements carried out every 1/2 hour. Each sample had 5000 events which allowed measuring the centroid to an accuracy of ≈ 0.2 channels. We notice an oscilation, with a period close to 24 hours and an amplitude of ± 5 channels, while the width is rather constant.

In order to determine the influence of the pedestal on the periodical variations mentioned above, we monitored simultaneously the lead-glass signal and its pedestal using the procedure of a second delayed gate, described in Section 2.5. As seen from Fig. 9, which shows the variation of the signal (a) and pedestal (c) over a period of ≈ 14 hours, the variations of the signal are significantly larger that those of the pedestal and should therefore be associated with the lead-glass detector. In Fig. 9 (b) and (d) we show the corresponding variation of the rms width of the signal and pedestal, respectively.

The most likely source of a ≈ 24 hour oscilation might be small temperature variations in the PC4 vault. We monitored the ADC spectra in parallel with the temperature of the Photon 4 calorimeter using the procedure described in Section 2.5. In Fig. 10, we compare the variation of the signal centroid (a) and pedestal centroid (b) with the temperature (c). In Fig. 11, we compare the corresponding rms widths. The temperature variation is only of $\approx 1^oC$. Both the average signal and pedestal seem to increase at lower temperature, where there is a small increase of the signal over the pedestal. The rms widths also may show a small increase at higher temperature. In Fig. 12 and 13 we present the same measurement extended over a longer time period.

The most likely candidate of a temperature correlated variation should be the LED output, but a variation of the phototube gain can not be ruled out at this stage. A way to check the phototube stability is to use a radioactive light pulser. We performed those tests at Tel-Aviv Univ. using an ^{241}Am light pulser and found the phototube stable to 0.2%, i.e. comparable with the observed variations. In this test (see Section 4 for more details), the voltage of the last 4 dynodes was not stabilized (no Magic box), we used a LeCroy HV4032A voltage supply (instead of the Fluke) and the variation of the room temperature was not monitored.

3.5 Pedestal noise

The pedestal noise is an important factor affecting the ultimate achievable energy resolution and must be minimized. In this section we discuss two different tests carried out during (i) August 1994 and (ii) September-December 1994. The first tests identified a quite large level of pedestal noise, while the second tests succeded to reduce it significantly. Although the first tests have been superseded by the second ones, we include them for reference.

3.5.1 August 1994 tests

As already mentioned in Section 3.2, the pedestal noise is rather large, and one must look for ways to reduce it. In order to determine the main source of noise, we monitored the signal spectrum over short ≈ 6 min periods in which we took 20 samples of 5000 events each. For each run we introduced a change in the system. In Table 2 we show the changes and the corresponding influence on the ADC spectrum.

Only in case 1 is there a signal, while in cases $2-5$ there is only the pedestal. Its dispersion increases if the grounding is bad (as in case 2 when the phototube high voltage cable was floating) and is not affected by changes of phototube voltage (case 3) or of LED operation (case 4). Finally, it decreases practically to zero if the ADC is isolated from the lead-glass (case 5). The pedestal dispersion is therefore due to electronic noise in the cable, which has also a DC component from the phototube (case 5).

One possible source of the electronic noise is 60 Hz pick-up and its harmonics in the cable, visible on the scope. In order to check this hypothesis, we compared signals taken simultaneously from two ADC channels. As seen in Fig. 14, there is a clear correlation, but not a strong one, indicating the existence of further sources of noise. The pedestal noise must be reduced by a more careful grounding of the entire system. With the ADC energy calibration mentioned in Section 1, this noise level corresponds to ≈ 400 MeV, while the goal is to have noise less than ~ 100 MeV.

Nr.	Change in the system	Pedestal spectrum	
		Average (channel)	Width rms (channel)
1	Normal: signal + pedestal	1386	13.8
2	Phototube voltage disconnected	1210	28.9
3	Phototube voltage down	1209	10.8
4	LED pulse amplitude down	1207	10.7
5	ADC terminated in 50 ohm	1190	0.6

Table 2: A few changes in the system and the corresponding modifications of the signal spectrum over short monitoring periods of ≈ 6 minutes.

Finally, we monitored simultaneously all 64 inputs of the ADC module over a period of ≈ 24 hours, taking each hour a sample of 5000 events in each ADC input. There were 2500 events for the signal and 2500 events for the pedestal. Only one ADC input was connected to a cable, the rest were open and unterminated.

In Fig. 15, we show the average pedestal (a) and its dispersion (b), in units of the ADC input number. We note large variations of the average pedestal of about ± 100 channels and also large variations of $1-10$ channels for the rms width. Among the 64 inputs, 26 inputs had numerically a rms width equal to 0.001 channels. Their correct operation should be checked.

3.5.2 September-December 1994 tests

These tests were carried out with essentially the same setup shown in Fig. 1, with the following differences:

- Eight ADC inputs were used, namely numbers $1-8$, and connected to eight lead-glass detectors.
- The phototube voltages were provided by the BPS.
- The grounding of the cables was redone by a more careful soldering.

After these changes, the 60 Hz mode was not visible on the scope any more, and the pedestal noise was significantly reduced.

In Fig. 16 we present the behaviour of the pedestal average (a) and rms width (b) for the first eight inputs of the 1881 ADC after these changes. By comparison with Fig. 15 we notice a significant reduction of the pedestal noise by approximately a factor of 3. Further effort was focussed on the remaining noise source. The technique of fast Fourier transform indicates the presence of a rather flat spectrum of frequencies, whose origin could not be identified.

In Fig. 16 we show two sets of measurements: the first one (open squares) was carried out as before, while during the second one (open circles) seven ADC inputs were correlated to the eighth. It was found that all ADC inputs belonging to a group of eight (there are four such groups) are correlated in amplitude. This technique allows to further reduce the pedestal noise, from 2.7 to 1.9 channels on the average, or by 26%; but has the drawback that it requires using one out of sixteen ADC inputs for this dedicated purpose.

In conclusion, after a more careful grounding of the system, the pedestal noise was reduced to 2.7 ADC channels, equivalent to an energy resolution of 6.5, 16.5 and 99.0 MeV in Photon 1,2 and 3/4 respectively.

4 Lead-glass linearity

The linear response of each lead-glass detector to the input light intensity in the photon calorimeter is essential, since the response should be proportional to the photon energy. A small non-linearity, in particular at high energy, may be tolerated; but it should be known in order to allow for corrections.

As mentioned in Section 3.3 we performed lead-glass linearity tests. They could not be done properly within the existing experimental setup, since the LED output was not proportional to the voltage input. In addition, the LED intensity was very small, of the order of 1 GeV equivalent energy.

In parallel with the activity at FNAL, lead-glass tests were carried out at Tel-Aviv Univ., using a very similar experimental setup, shown in Fig. 17. As a light source, we used a red LED and a blue laser, whose pulse intensities could be precisely attenuated using calibrated neutral density filters [8]. The phototube signal was integrated in the 11-bit (2048-channel) 2249w ADC, which has a maximal range of 512 pC, and using a 100 nsec. gate. These tests were carried out to date without voltage stabilization (without Zener diodes) on the last 4 dynodes of the phototube.

In order to extend our measurements to the necessary equivalent energy range of ≈ 40 MeV to ≈ 500 GeV, we used the following procedure:

(i) for energies lower than the ADC resolution, we raised the phototube voltage and then we normalized the measurements at a point common for both voltages,

(ii) for energies higher than the ADC range, we reduced the signal using an attenuator, and we used its calibration to compute the correct charge.

In order to enhance the number of energy points, we combined the filters in all possible ways. When $2-4$ filters were combined, we noticed a small systematic increase of the actual transmission relative to the product of the intrinsic transmissions, probably due to multiple reflections.

The results of our measurements are shown in Fig. 18 and 19, where we plot the phototube charge as a function of the equivalent energy, for several phototube voltages, and for two extreme energy ranges: low energy up to ≈ 12 GeV and high energy extending beyond 500 GeV respectively. The energy scale was fixed using a previous lead-glass calibration with 30 GeV electrons [9], in which $\approx$ 24 GeV equivalent energy was contained in an average lead-glass block, while the measured ADC charge was $\approx$ 250 pC at a phototube voltage of -1100 V. We note that for typical voltages of $1000 - 1400$ V the lead-glass response is linear at lower energy, but shows significant non-linearity above $\sim$ 100 GeV. We also observe that at these energies, the charge output exceeds the 400 pC range of the 1881M ADC designed for the E781 experiment. A more detailed discussion of the lead-glass response will be given in [7].

5 Conclusions

This report summarizes results of the first readout tests of an E781 photon calorimeter carried out during August 1994 at FNAL. We used a single lead-glass detector of the Photon 4 calorimeter and the essentials of the anticipated complete readout system, including 66 m long cables, the prototype 1881 ADC, FASTBUS and a simple C-code running under the VxWorks operating system on a FSCC computer. The data analysis was performed on the FN781A (Challenge) host computer.

As light source, we used a green LED coupled to a bundle of optical fibers, located on the front plane of the calorimeter. The LED was fired from upstream by 30-100 nsec pulses, with an aplitude of +5 V, at a rate of 1 kHz, via a $\approx$ 66 m cable. The light pulses were injected via optical fibers into the front end of a lead-glass counter, readout by a FEU-84-3 phototube, operated at a high voltage of -1500 V. The phototube signals, transported back upsteam by a $\approx$ 66 m cable were integrated in the ADC using a 100 nsec. gate. We measured the lead-glass signal using the ADC input numbers $1 - 3$ and 14 and the pedestals of all the 64 inputs.

Using this system, we studied the lead-glass signal and pedestal stability for different ADC inputs, over monitoring periods of $1-3$ days. We found $\approx$ 24 hour signal variations of a few ADC channels, apparently related to LED output changes due to $\approx 1^o$ temperature day-night variation in the PC4 vault. The intrinsic LED pulse-to-pulse dispersion was $\approx 4\%$.

The ADC pedestals are apparently less affected by these changes. They have average values of $\approx$ 1200 channels, a variation of approximately ± 100 channels between different ADC inputs and pulse-to-pulse rms variations of $\approx$ 10 channels. The long range variations of the average pedestal is $1-2$ channels. Both the signal and the pedestal seem to increase slightly when the temperature decreases.

The pedestal dispersion is likely associated with the electronic noise in the cables. One source of noise is 60 Hz pick-up and its harmonics, which results in correlated noise between the ADC channels.

Work on further reducing the ADC pedestal noise was continued during September-December 1994. After a more careful grounding of the system and some other changes, the pedestal noise was reduced by approximately a factor of 3, namely to 2.7 channels on the average. This is equivalent to a present energy resolution of 6.5, 16.5 and 99.0 MeV in Photon 1,2 and 3/4 respectively.

We also report on the lead-glass response to various light levels in the range of 12, 50 and 500 GeV equivalent energy, and for several phototube voltages. We found a linear response for low energies and significant non-linearity for energies above ~ 100 GeV.

In conclusion, the complete readout chain of a single channel of the Photon 4 calorimeter is operational. This creates the basic framework for the development of the complex harware/software instrumentation of the four E781 photon calorimeters.

Acknowledgements

During this work we received assistance from many of our E781 colleagues to whom we express our gratitude. We thank F. Pearson for producing the signal cables and D. Northacker for installing them in PC4. Both provided friendly help on many other occasions. We thank L. Stutte, M. Kubantsev and L. Landsberg for valuable remarks on the design of the laser monitor system. We are grateful to M. Balatz and M. Zilka for their contribution to the Tel Aviv tests.

This work was supported in part by the U.S.-Israel Binational Science Foundation, Jerusalem.

Appendix – Software

The software related to ADC readout resides in the directory */home/gerzon/adc* in the Challenge FN781A computer. It consists basically in three programs: the data acquisition C-code *vstab.c* (and its versions *mstab.c* or *two.c*, etc.) and the data analysis fortran codes *hmao.f* and *hmao2.f*.

We advice you to create (starting from your *home* directory) a subdirectory named *adc*. Then, you may copy our entire */home/gerzon/adc* directory to yours. You will also have to replace in the codes *hmao.f* and *hmao2.f* the name *gerzon* with yours.

In order to work, you need some basic knowlege of the 1881 ADC [1], the FSCC operating system VxWorks [11] and Fastbus [12]. Our experience is summarized at the end of this appendix.

In order to compile the *vstab.c* program you use the makefile *makeo* (which exists in the */home/gerzon/adc* directory) by the command *makeo vstab.c*. This creates the object file *vstab.o*.

In order to run your program you first login to the FSCC computer located in the crate where the ADC resides. For example, in order to login to *fb781a*, you type *rlogin fb781a* and then you answer the user *ID* question as *VxWorks* and the password *PW* question. Then you go to your working directory by typing *cd "/home/your_name/adc"* (don't forget the "). In order to load your program, type *ld < vstab.o*. Then, type *vstab* in order to run it. In order to exit from the FSCC, type *logout*.

Data acquisition

In order to read the ADC, we used the program *vstab.c* which runs in the FSCC under VxWorks operating system. The C-compiled module is called *vstab.o*.

The program reads data from one ADC input connected to a lead-glass block. The other inputs, which have only pedestals may be supressed by setting a threshold or may be readout as well by lowering the threshold. This threshold is the "zero suppression" facility of the ADC, by which one avoids reading empty ADC inputs. The program collects a specified number of events and then writes them to an ascii file which will contain a spectrum. Then the program waits a specified number of seconds and takes the next sample of events. Finally, you will have in your *adc* directory the spectra files *histi*, where *i* is the measurement number. The running conditions and a short summary are contained in the file *gtest.log*.

At the start, the program asks for the running conditions:

– the slot number of the FASTBUS crate where the ADC module resides,

– the ADC input number which has signal,

– the threshold (in channels) which you set for the signal (in order to suppress the pedestals),

– the ADC input number without threshold (unsuppressed),

– the number of events per measurement,

– the number of measurements,

– the waiting time (in seconds) between the measurements.

The program may be run interactively or may be submitted in background (see [11]) for longer monitoring periods.

A more complex version of *vstab.c* is the program *mstab.c* which monitors simultaneously all the 64 ADC inputs. For each input the program monitors both the signal and the pedestal. This program produces the file *mstab.stat*. This file contains, for each measurement and for each of the 64 ADC inputs: the number of events, the average and the rms width for both the signal and the pedestal spectrum. In order to separate the signal and the pedestal spectra for the calculation of the average and rms width, a channel number separating them must also be given.

Finally, we mention the program *two.c* which monitors two ADC inputs and writes to disk their spectra in the file *chi_j*, where i is the ADC input number and j is the measurement number.

Data analysis

The programs *hmao.f* and *hmao2.f* read the ascii files produced by *vstab.c* and *mstab.c*, construct histograms and write them to a histogram file. They may be run by typing *hmao* and *hmao2* respectively.

The program *hmao* was used when we measured only the signal from the lead-glass. It constructs histograms for:

– the ADC spectrum for each measurement,

– the integral spectrum over all measurements,

– the monitoring of the mean and rms width of those spectra as a function of the measurement number.

The program *hmao2* was used when we measured both the signal and the pedestal for each ADC input by the delayed gate method. This program constructs the histograms mentioned above for both the signal and the pedestal.

For example, in order to run *hmao2* you simply type *hmao2*. The program asks a few questions which you answer as follows:

choose directory → The answer must be *adc*.

choose number of files → Type the number of measurements you made.

choose separation point → type an ADC channel number between the expected signal and pedestal peaks. For example, if the pedestal is centered around channel 1200 and the signal around channel 1500, you may type 1350.

The constructed histograms will be written on the RZ file *adctest.his*, which may be opened and read by PAW. Further they may be modified and plotted in PS format. Finally, the PS file may be printed on a PostScript printer.

Temperature monitoring

The monitoring of the temperature inside Photon 4 is carried out by running the program *sad_example.c* which resides in the directory */home/steiner/epicure*. Information on this code may be found in the file *sad.doc* or from Ed Dambic (phone 2465). One starts the temperature monitoring by typing *sad_example dale* > & *temp* &.

Presently, the program reads the temperature sensor number 3 from the PC4 vault, namely PC4TEMP3, every 300 seconds. The temperature monitoring is therefore independent on the ADC monitoring. As a next development, it would be useful to do it at the same time with the ADC readout, by including *sad_example.c*, as a rountine, in the ADC monitoring code.

Sample code of the ADC monitoring

As an example, we include the list of the code */home/gerzon/adc/vstab.c*:

```
#define DEBUG 1
#include "math.h"
#include "stdioLib.h"
#include "fb_parm.h"
#include "adc_utils.h"

#define NUM_CHANNEL 64
#define DATABUFSIZE 256

float mean[100], stddev[100] ,std, std1;

int vstab()

/* nc = number of events nedeed
ach = adc channel
ch_npds = channel number without threshold
thr_val = threshold */
{
FB_word pa = 23 ;
int nc=1000, ach=1, ch_npds=1, thr_val=1000 ;
char gcur ;

int igg = 1 , imax = 24 , gdelay = 1800 ;
char gbb[5];

FB_word rbuf[DATABUFSIZE];
int i,j,read_ptr,write_ptr,num_ch,thrs[NUM_CHANNEL];
int curev=1;
adc_event_data dataword;

FILE *histogram_file, *rep_file ;
char *fn="hist", *fn1="gtest.log" ;

rep_file = fopen (fn1,"w");
if (rep_file == NULL)
{
```

```
    printf("Open file error file name %s \n",fn1);

    return(-1);
}
printf("\n strike return");
gcur = getchar();
printf("\n Do you like to change anything ? ");
gcur = getchar();
if(gcur =='Y' || gcur =='y')
{
printf("\n ADC slot ? =");
do scanf("%d", &pa) ;
while (pa < 0 || pa > 25) ;

    printf("\n number of events ? =");
do scanf("%d", &nc) ;
while (nc < 1 || nc > 1000000) ;

    printf("\n ADC channel ? ");
do scanf("%d", &ach) ;
while (ach < 0 || ach > 63) ;

    printf("\n threshold ? ");
do scanf("%d", &thr_val) ;
while (thr_val < 0 || thr_val > 8191) ;

    printf("\n ADC channel without threshold? ");
do scanf("%d", &ch_npds) ;
while (ch_npds < 0 || ch_npds > 63) ;
printf("\n number of measurements ? ");
do scanf("%d", &imax) ;
while (imax < 1 || imax > 20000) ;
printf("\n time between measurements ? ");
do scanf("%d", &gdelay) ;
while (gdelay < 0 || gdelay > 20000) ;
}
printf("\n ADC slot = %d", pa);
printf("\n number of events = %d", nc);
printf("\n ADC channel = %d", ach);
printf("\n threshold = %d", thr_val);
printf("\n ADC channel without threshold is %d", ch_npds);
printf("\n number of measurements is %d ", imax);
printf("\n time between measurements is %d sec.", gdelay);
printf("\n\n\n");
```

```
fprintf(rep_file,"\n ADC slot = %d", pa);
fprintf(rep_file,"\n number of events = %d", nc);
fprintf(rep_file,"\n ADC channel = %d", ach);
fprintf(rep_file,"\n threshold = %d", thr_val);
fprintf(rep_file,"\n ADC channel without threshold is %d", ch_npds);
fprintf(rep_file,"\n number of measurements is %d ", imax);
fprintf(rep_file,"\n time between measurements is %d sec.", gdelay);
fprintf(rep_file,"\n\n\n");

initial_port();
set_oport_parm(FB_OPORT_FORCE_EVENT);

fprintf(rep_file,"\n measurement number mean stddev\n\n");

for(igg =1;igg <= imax;igg++)
{
mean[igg] = 0. ;
stddev[igg] = 0. ;
sprintf(gbb,"%s%d", fn, igg);
histogram_file = fopen (gbb,"w");
if (histogram_file == NULL)
{
printf("Open file error file name %s \n",fn);
return(-1);
}

for(i=0; i < NUM_CHANNEL;i++)thrs[i]=thr_val;
thrs[ch_npds]=0;
/* fprintf(rep_file,"ID of adc in slot %2d: %4x\n",
pa,adc_read_adcidwd(pa)); */

adc_write_cword0(pa,ADC_WR_MREST);
adc_write_cword0(pa,ADC_WR_FSCLR);
adc_write_cword1(pa, ADC_WR_13bit|ADC_WR_FCW14|ADC_WR_ENSPA) ;
for(i=0; i < NUM_CHANNEL;i++)
adc_write_thr(pa, i, thrs[i]);
adc_write_cword0(pa,ADC_WR_ENWAI|ADC_WR_ENGAT|ADC_WR_RSERR|ADC_WR_DSLAD);
write_ptr=0;
curev = 1;
while(curev <= nc)
{
while(write_ptr!=curev%64)
adc_read_pointer(pa,&read_ptr,&write_ptr);

/* printf("this is write pointer %d\n",write_ptr);
```

```
printf("this is read pointer %d\n",read_ptr);
/ adc_write_cword0(pa,ADC_WR_LNEVE );
adc_read_datword( pa, &dataword);
/* fprintf(rep_file,"%d this is data header %d %d\n",
i,dataword.hdwd.evid, dataword.hdwd.nchs); */
for(j=0; j < dataword.hdwd.nchs;j++) {
/* fprintf(rep_file,"this is the content of the channel %2d :%4d\n",
dataword.dtwd[j].chid,dataword.dtwd[j].data); */

    /* fill hist for channel ach */
if(dataword.dtwd[j].chid == ach) {
fprintf (histogram_file, "%d\n",dataword.dtwd[j].data);
mean[igg] += dataword.dtwd[j].data ;
stddev[igg] += dataword.dtwd[j].data * dataword.dtwd[j].data ;
}
}
curev++ ;
}

    mean[igg] /= nc ;
stddev[igg] /= nc ;
stddev[igg] = stddev[igg] - mean[igg]*mean[igg] ;

    std1 = stddev[igg];
if(std1 <= 0.) std1 = 0. ;
std = sqrtf(std1) ;
stddev[igg] = std ;

    fprintf(rep_file," %d %f %f \n",
igg, mean[igg] , stddev[igg]) ;

    adc_write_cword0(pa,ADC_WR_DSGAT);
i= fclose (histogram_file);
taskDelay( gdelay * sysClkRateGet() ) ;
}
i= fclose (rep_file);
set_oport_parm(FB_OPORT_HOLD);
close_port();
return(0);

    } /* adc_cbltest end */

    #if 0
```

```
#define ADC_WR_STERR 0x00000001 /* set error flag */
#define ADC_WR_ENLAD 0x00000002 /* set logical address enable */
#define ADC_WR_ENGAT 0x00000004 /* set gate enable */
#define ADC_WR_MREST 0x40000000 /* master reset */
#define ADC_WR_FSCLR 0x80000000 /* fast clear pulse */
#define ADC_WR_13bit 0x00000040 /* 13 bits ADC */
#define ADC_WR_ENSPA 0x40000000 /* enable sparsification */
#define ADC_WR_FCW14 0x06000000 /* fc window width */
#define ADC_TH_ADDRS 0xc0000000 /* address of threshold register */

#endif
```

Some hints about getting started with FSCC, VxWorks and Fastbus

The information contained in this section was valid during August 1994. At the release date of this report, the on/off line shell running on the FSCC was still being developed and important changes (for example, implementing DART software) are expected soon. The computer experts should be consulted before starting the work [10]. However, we included in this report our experience since it may be helpful on the short time scale.

The Fastbus Smart Crate Controller (FSCC) is a computer running the real-time operating system VxWorks [11].

The executable programs (C-compiled and linked) are produced on the E781 host fn781a computer (Challenge Silicon Graphics with Unix operating system). Then, they are loaded to the FSCC for execution.

The shell on fn781a is bash (Bourne again shell), so the name of your file for the definition of environment and aliases is *.bashrc* instead of *.cshrc*. Examples of .bashrc file are: */home/jurgen/.bashrc* and */home/gerzon/.bashrc*

It's nice to have in your .bashrc at least the following lines:

setup edt

export TERM="vt100"

setup cern (which includes PAW and PAW++)

setup vx_fscc

setup -f VxWorks fb_fscc

setup -f VxWorks fb_std

The cc68k cross compiler (C-compiler to generate code for VxWorks targets) is used for compilation of every C-source. You can use the makefile it /home/gerzon/adc/makeo to compile a C-source code to produce an object file.

Example: *makeo filename.c.*

There is also C++ cross compiler, whose name is *CC68k*. For more information type: *man cc68k*.

If a program has several modules, after compilation you must link them (on fn781a) with the *ld68k* linker.

Example: *ld68k -o applic.o -r applic1.o applic2.o applic3.o*

This command creates one executable *applic.o* file from the files *applic1.o, applic2.o, and applic3.o*.

For those who prefer to use the *make* procedure, there is an example of a *Makefile*, residing in the directory */home/svoiski/fsda/proj* on the fn781a.

After producing an executable file on the fn781a you go to the FSCC using the *rlogin* procedure:

Example: *rlogin fb781a*

At the login prompt, you answer for the user id: *VxWorks* and then you give the password (get it from another user).

Now you are in the directory which is defined in start-up script. Start-up scripts reside in the directory */home/vxworks/scripts*.

The command *help* gives you a list of VxWorks commands with parameters and options.

You can change directory with the command *cd "your_new_directory"* (do not forget the "..." quote signs).

The command *ld < prog.o* loads a program from disk to FSCC memory.

To run a program just type: *program_name(param1, param2, ...)*.

The command *lkup "symbol"* list symbols from system symbol table (do not forget the "..." quotes), and the commands *ls* and *ll* list the contents of a directory.

The commands *sp* and *taskSpawn* spawn a task (similar to background jobs in Unix).

In order to exit from FSCC, type *logout*.

The work with Fastbus requires the Fastbus Standard Routines (FSR) package. (see User's Guide for C/VxWorks FASTBUS Standard Routines - Fermilab document PN463).

There are also *man* pages for FSR on the fn781a. As an example, type: *man fbopen*.

You can look at the *man* pages yourself by typing:

/home/dnmao/man/lst - list of mans and cats

/usr/products/man

/usr/products/vxworks/vxworks/v2_0/man

Important directories containing routines and header **.h* files for work with Fastbus from FSCC are:

FB_FSCC_DIR=/usr/products/vxworks/fb_fscc/v2_0

FB_STD_DIR=/usr/products/vxworks/fb_std/v2_0

This is a sample subroutine to write a command to the 1881 ADC control register *csr0*:

```
void adc_write_cword0(FB_word pa, FB_word control_word)

BUS_ARBITRATE(8);
ADDRESS_CSR_GEOGRAPHICAL(pa); /* slot number */
DATA_SEC_ADDRESS_WRITE(ADC_CSR0); /* register */
DATA_RANDOM_WRITE(control_word);
ADDRESS_RELEASE;
BUS_RELEASE;
```

Useful macros which were used above are defined in the file:

/usr/products/vxworks/fb_fscc/v2_0/include/fb_fscc_def.h

Examples of programs using FSCC and Fastbus are in the directories:

/data02/dnmao/fscc/tdc
/home/svoiski/fsda/proj
/home/gerzon/adc

There is a program for Fastbus tests called *fsrtk*. It is located in the directory

/usr/products/IRIX/fb_std/v2_1/bin.

In order to run it from fn781a, just type:

setup fb_std
fsrtk

The source of the program *fstrk* and some other source files are available in in the directory */usr/products/IRIX/fb_std/v2_1/src.* The *fstrk* opens windows and asks the FSCC name you need to connect to. You print, for example, fb781a in the upper bar, then click on Open button. The connection will be established. There is also a help button. Then, in the Fastbus transaction routines window you can execute various operations with Fastbus, like read and write to the control and data registers.

Finally, here is an example for ADC Control register 0 reading:

primary address = 23,
secondary address = 0,
buffer mode = variable,
settings = CSRSPACE private single.

Click on Fastbus *read* and you will read the content of the register.

References

[1] LeCroy model 1881M 64 channel FASTBUS ADC, July 1, 1994.

[2] green LED, type AND190GCP, 10 mm package, I(MCD@20mA)=1300, view angle 4°, stock number 50F3824, manufactured by Hewlet Packard, purchased from Newark Electronics, 625 Plainfield Rd. Willowbrook IL 60521.

[3] red LED, type AND190GRP, 10 mm package, I(MCD@20mA)=13000, view angle 4°, stock number 50F3823, manufactured by Hewlet Packard, purchased from Newark Electronics, 625 Plainfield Rd. Willowbrook IL 60521.

[4] The Photon $3/3'$ Trigger System of Experiment E-781, Yu.M. Goncharenko, O.A. Grachov, S.B. Nurushev, Fermilab H-note 683, May 10, 1994.

[5] Booster Power Supply of Photon Detectors PH3/4 of Experiment E-781, Yu.M. Goncharenko, O.A. Grachov, S.B. Nurushev, FNAL E781 H-Note, June 20, 1994.

[6] S.B. Nurushev, IHEP, Protvino, Russia, private communication.

[7] M.A. Moinester et al., The E781 Calorimeter Light Pulse System, FNAL E781 note H688, June 1994.

[8] Melles Griot, Optics Guide, 1988, pag. 11-22.

[9] S.B. Nurushev, IHEP, Protvino, Russia, private communication.

[10] J. Engelfried and D. Mao, VxWorks, FSCC, Fastbus, H-note, in preparation.

[11] For documentation on VxWorks, see e.g.:

VxWorks Programmer's guide - operating system manual
VxGDB User's guide - debugger manual

[12] IEEE Standard FASTBUS Modular High-Speed Data Acquisition and Control System, The Institute of Electrical and Electronics Engineers, 1985.

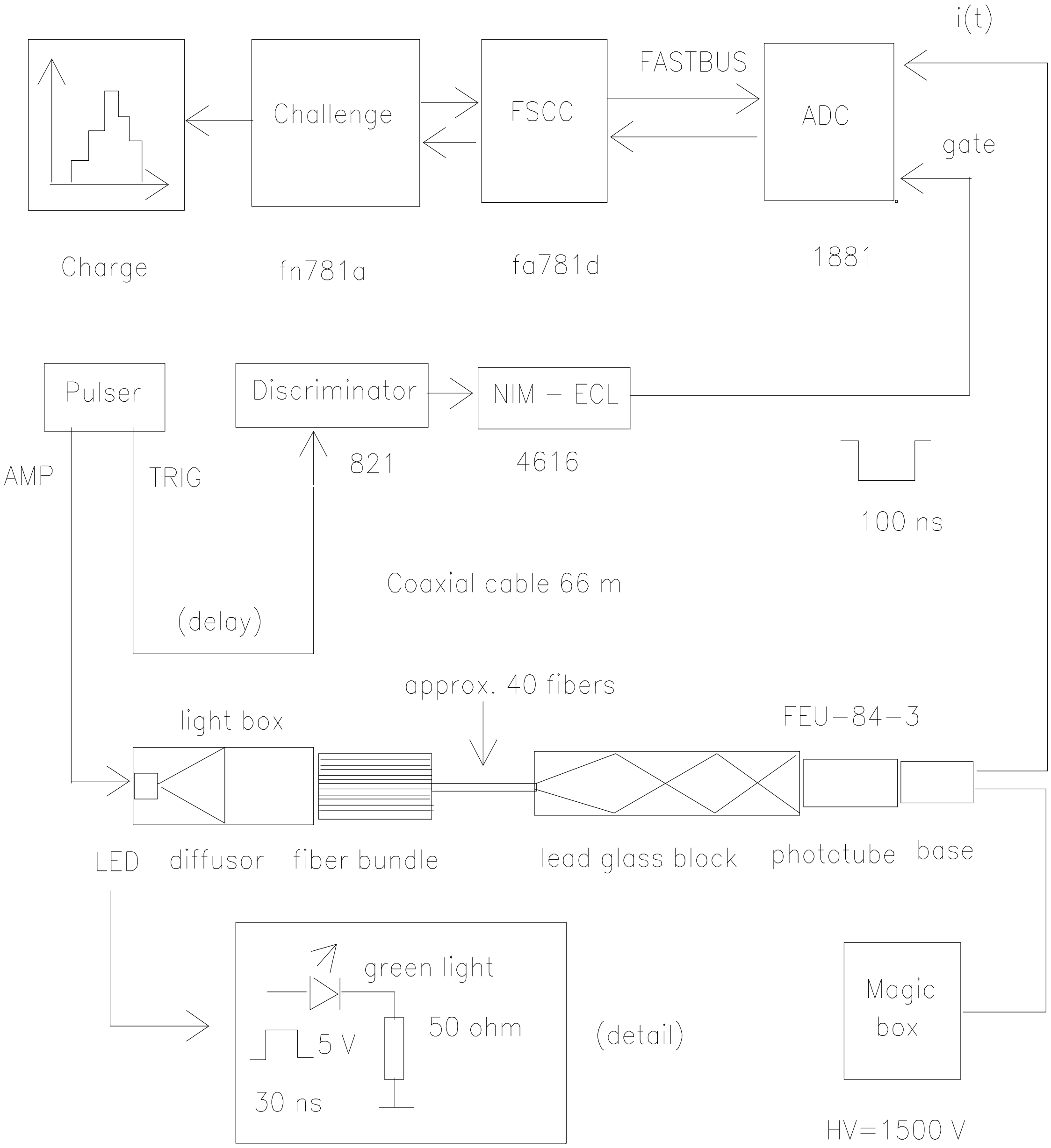

Figure 1: Basic experimental setup used during the August 1994 readout tests of channel 22115 of the Photon 4 calorimeter at FNAL.

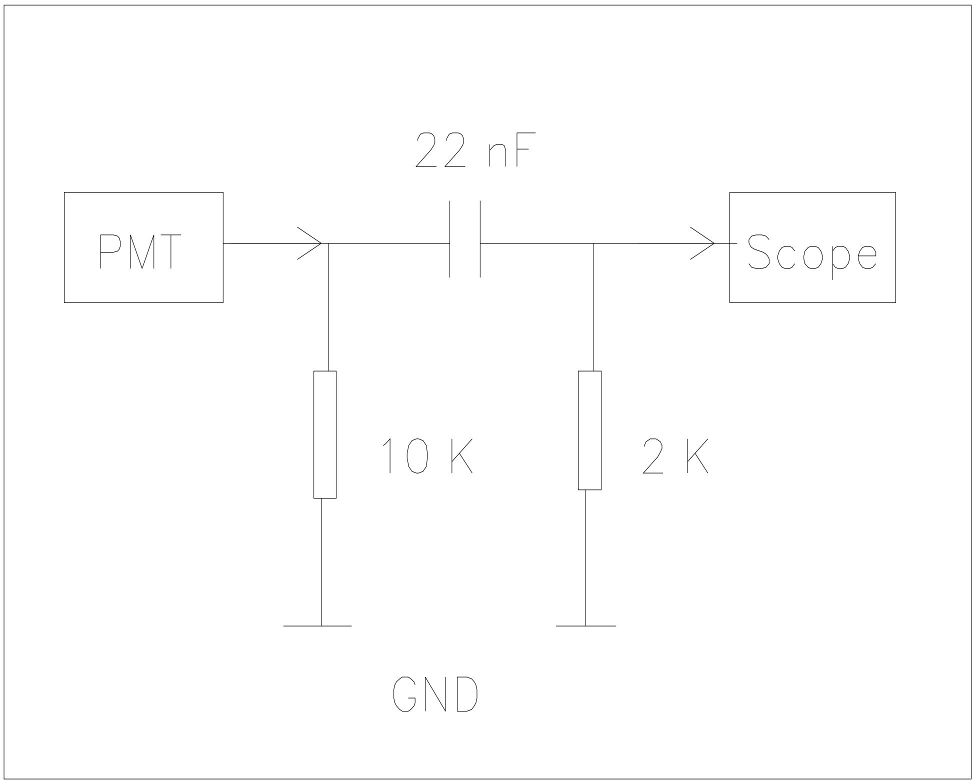

Figure 2: The circuit used for the measurements of illumination over the fiber bundle area. This circuit allows to filter out the low frequency noise due to the neon lights in the room.

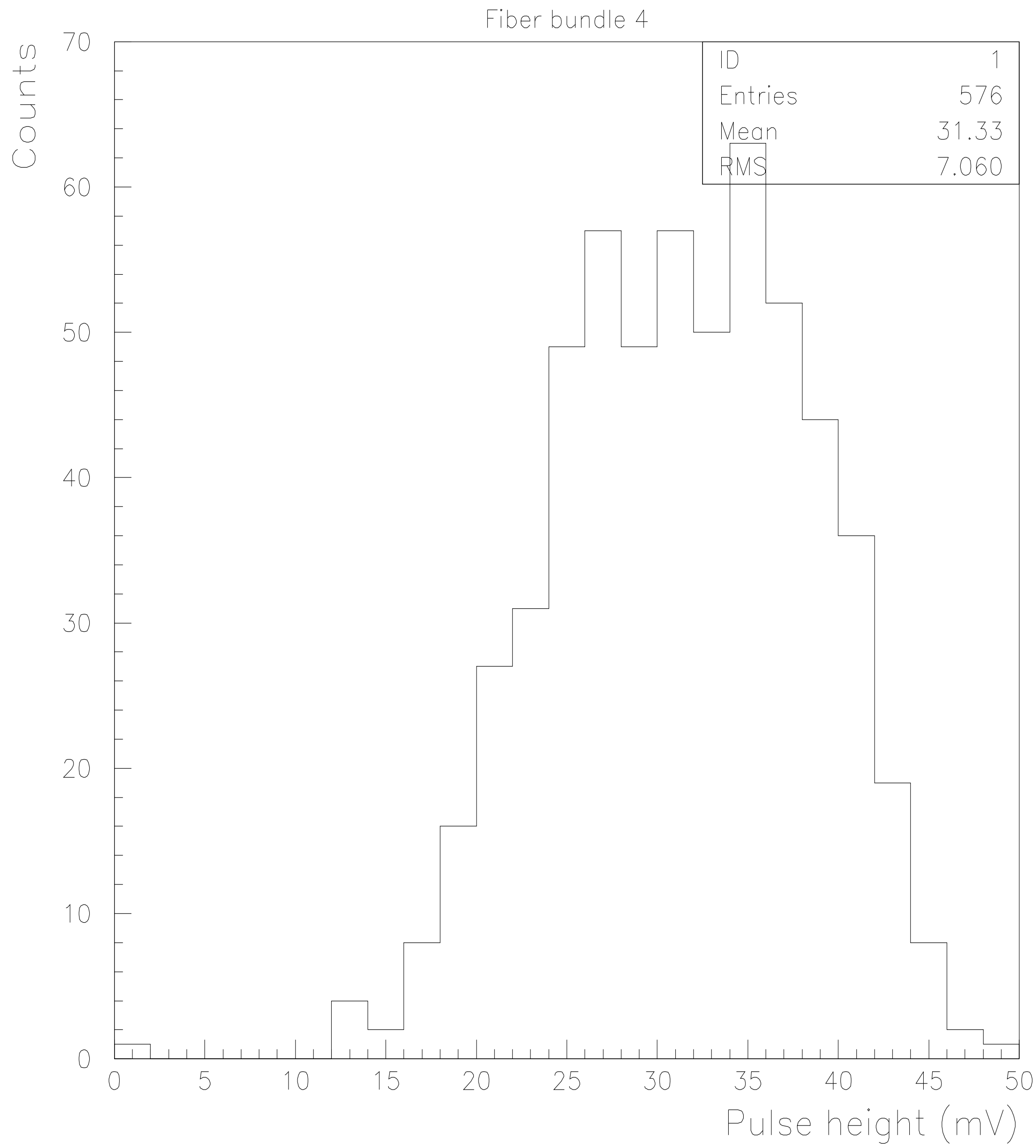

Figure 3: Uniformity of LED light illumination over the area of the fiber bundle in the light box, as measured by the pulse height distribution of signals from a FEU-84-3 phototube coupled to each fiber in the bundle. The attenuation of green light in the plastic fibers with variable lengths of $\approx 20 - 80$ cm is negligible.

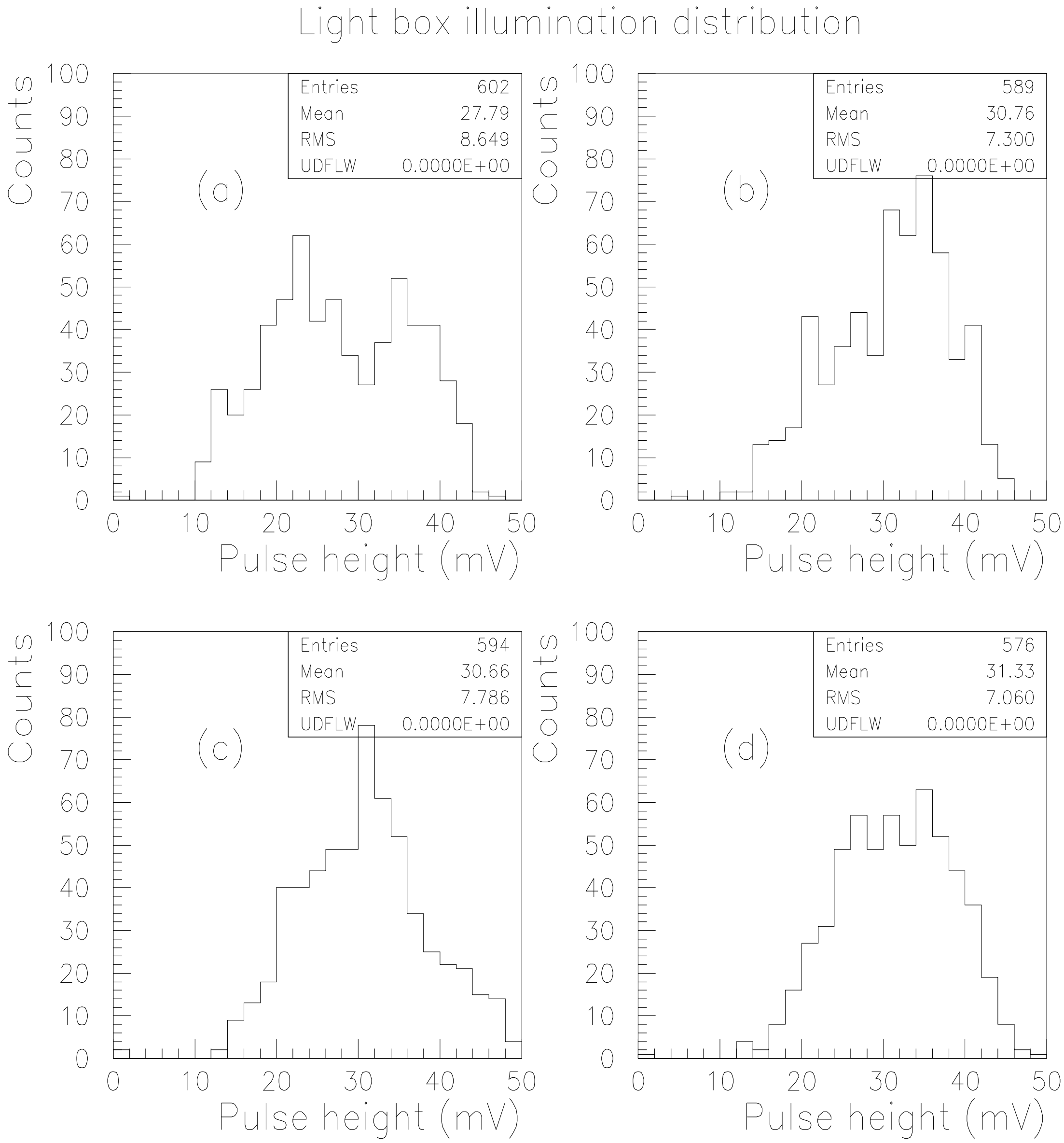

Figure 4: Comparison of the variation of light illumination over the surface of the fiber bundle, in the case of four different bundles. See Fig. 3 and the text for more explainations.

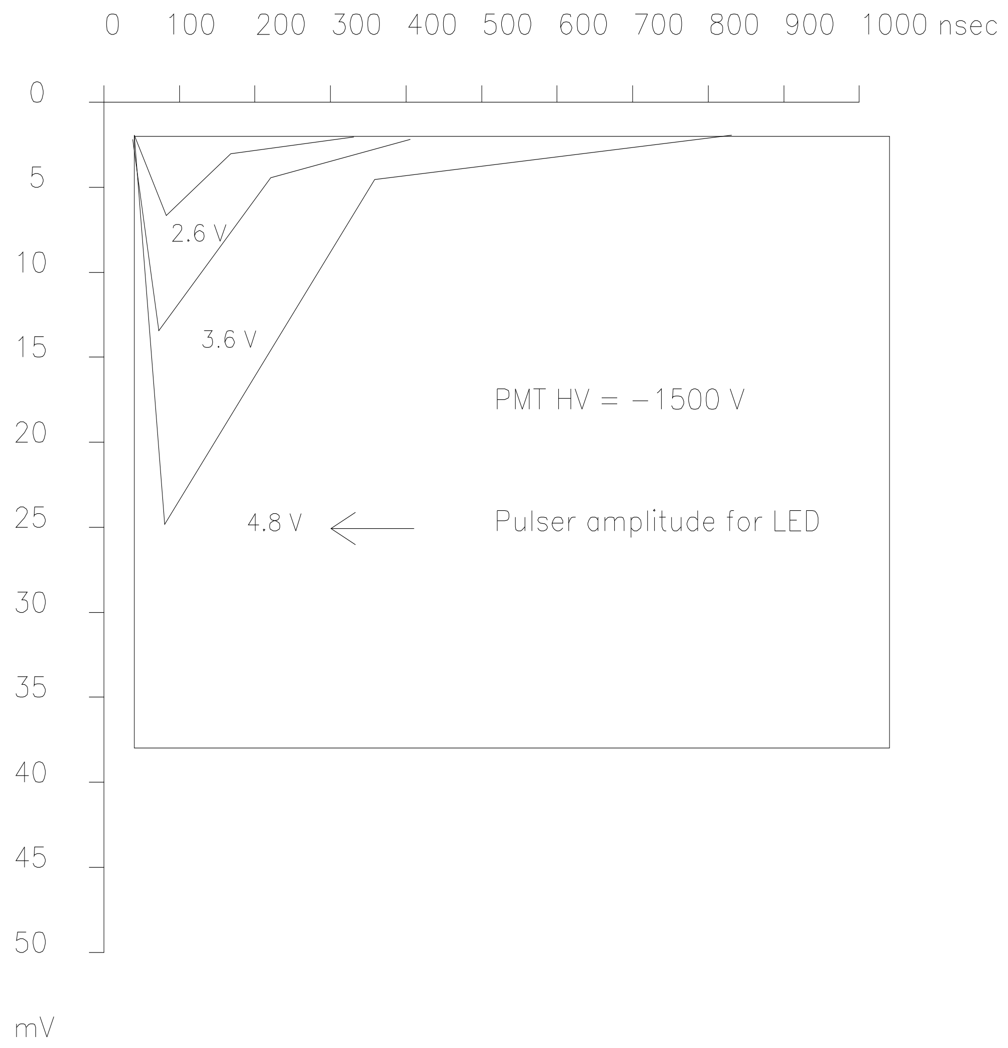

Figure 5: Schematic response of a lead-glass counter to a green LED pulse for phototube high voltage of -1500 V. The LED was fired by square pulses with amplitudes of 2.6, 3.6 and 4.8 V, width of 30 nsec, and repetition rate 1 kHz.

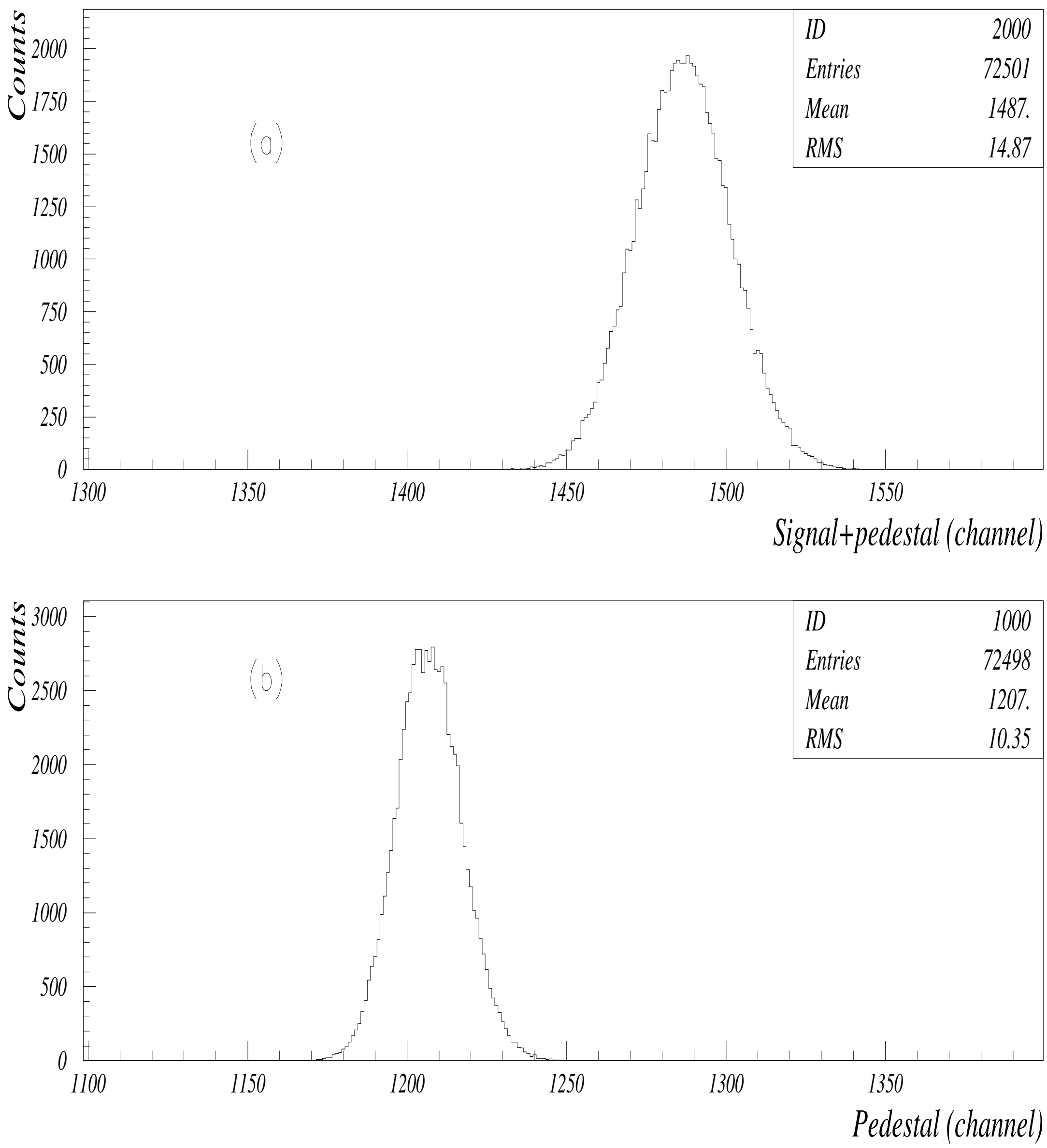

Figure 6: Typical spectra of the 22115 lead-glass detector: (a) signal + pedestal, (b) pedestal only. The LED was fired by a square pulse, 100 nsec long, with an amplitude of +5 V, at a rate of 1 kHz. The phototube high voltage was −1500 V. The phototube signal was directly fed to input number 1 of the 1881 ADC together with a 100 nsec gate.

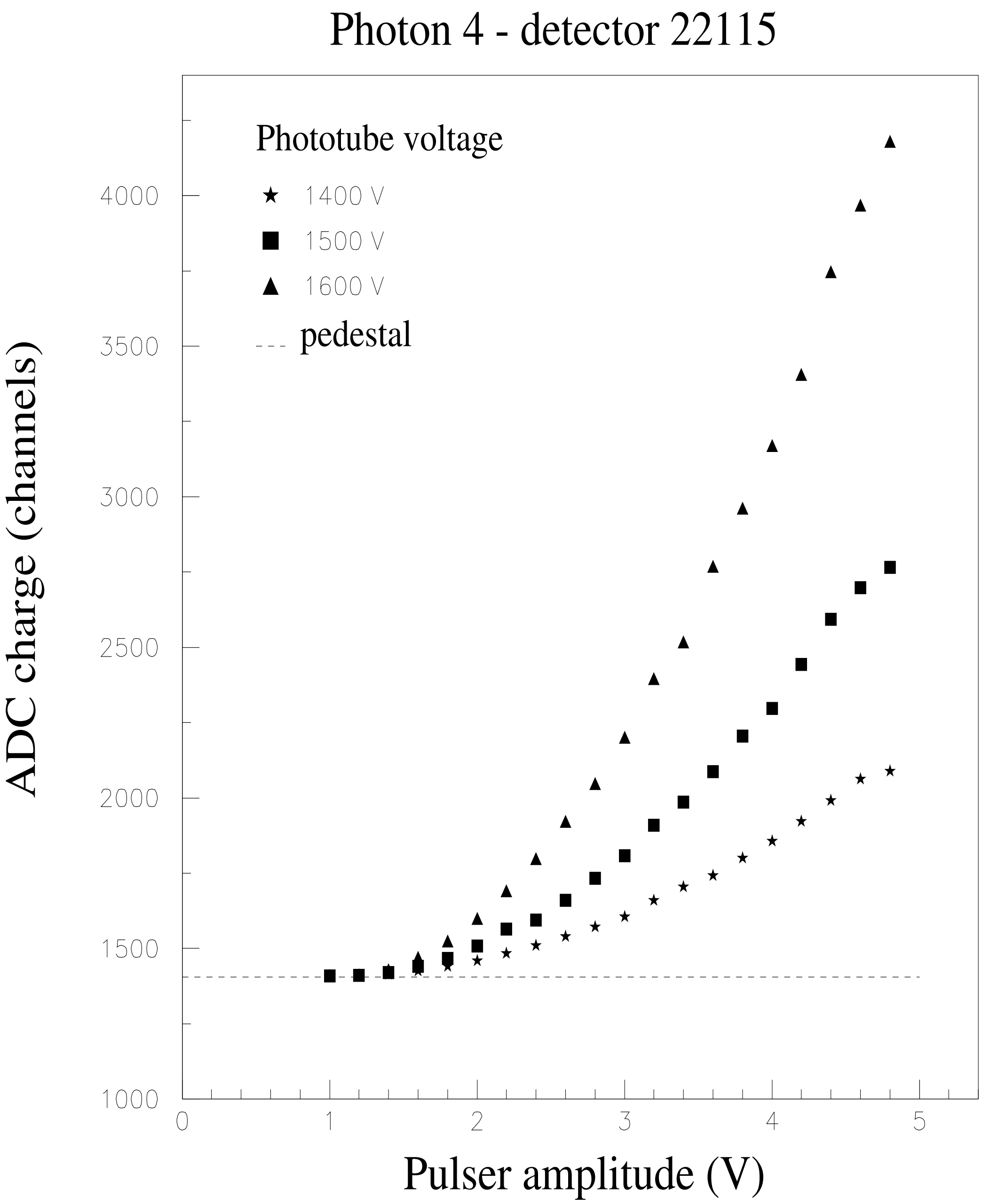

Figure 7: The response of the lead-glass to input LED pulse height for several phototube voltages. The LED was fired by a square pulse, 30 nsec long at a rate of 1 kHz. The phototube signal was directly fed to input number 1 of the 1881 ADC, together with a 500 nsec gate. As expected, the response is non-linear, since the LED light output is not linear with respect to the input voltage pulse height.

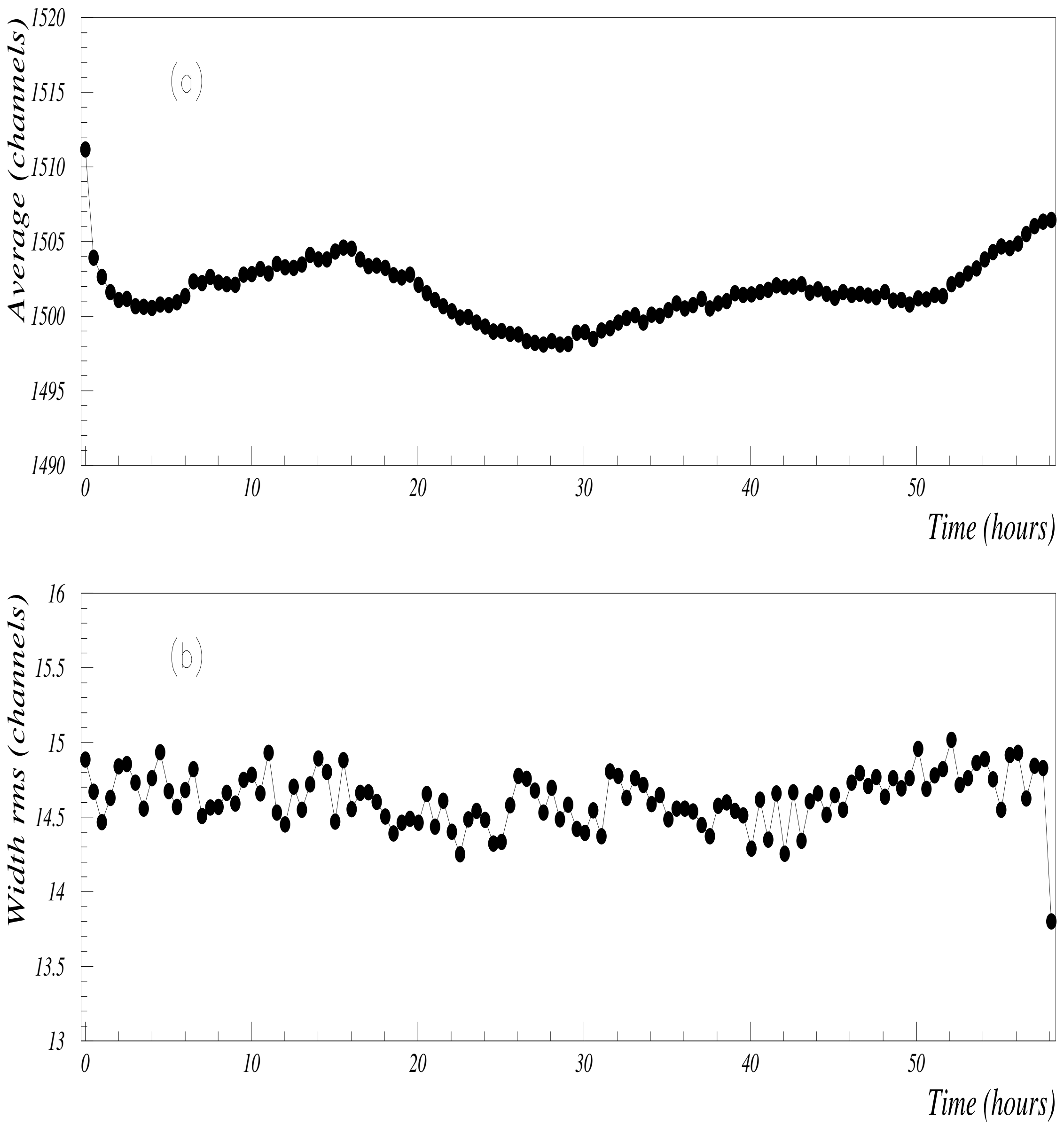

Figure 8: Variation of the signal spectrum centroid (a) and rms width (b) during 64 hours of continuous monitoring. Each sample contained 5000 events. The LED was triggered by a 30 nsec pulse of +5 V at a repetition rate of 1 kHz. The phototube voltage was −1500 V. The ADC gate was 100 nsec. We notice clear oscilations with a period of ≈ 24 hours.

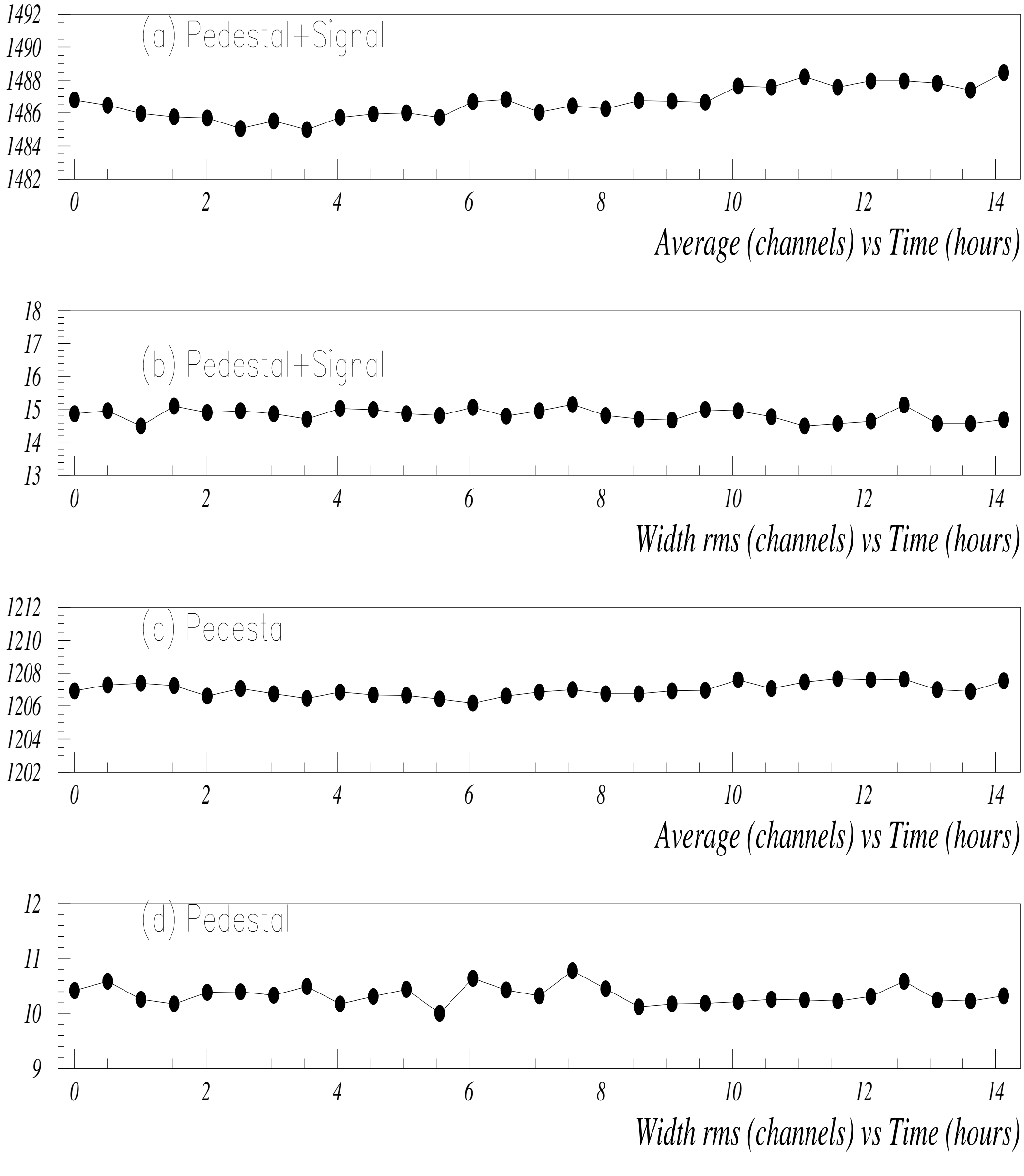

Figure 9: Variation of the centroids of the signal (a) and pedestal (c), as well as the rms width of the signal (b) and pedestal (d) during $\approx$ 14 hours of continuous monitoring. Each sample contained 5000 events. The lead-glass signal was connected to ADC channel number 1. The LED was triggered by a 30 nsec pulse of +5 V at a repetition rate of 1 kHz. The phototube voltage was −1500 V. The ADC input was number 3, and the gate was 100 nsec. We notice a clear increase of the average signal over the pedestal. The corresponding widths also show an increase trend.

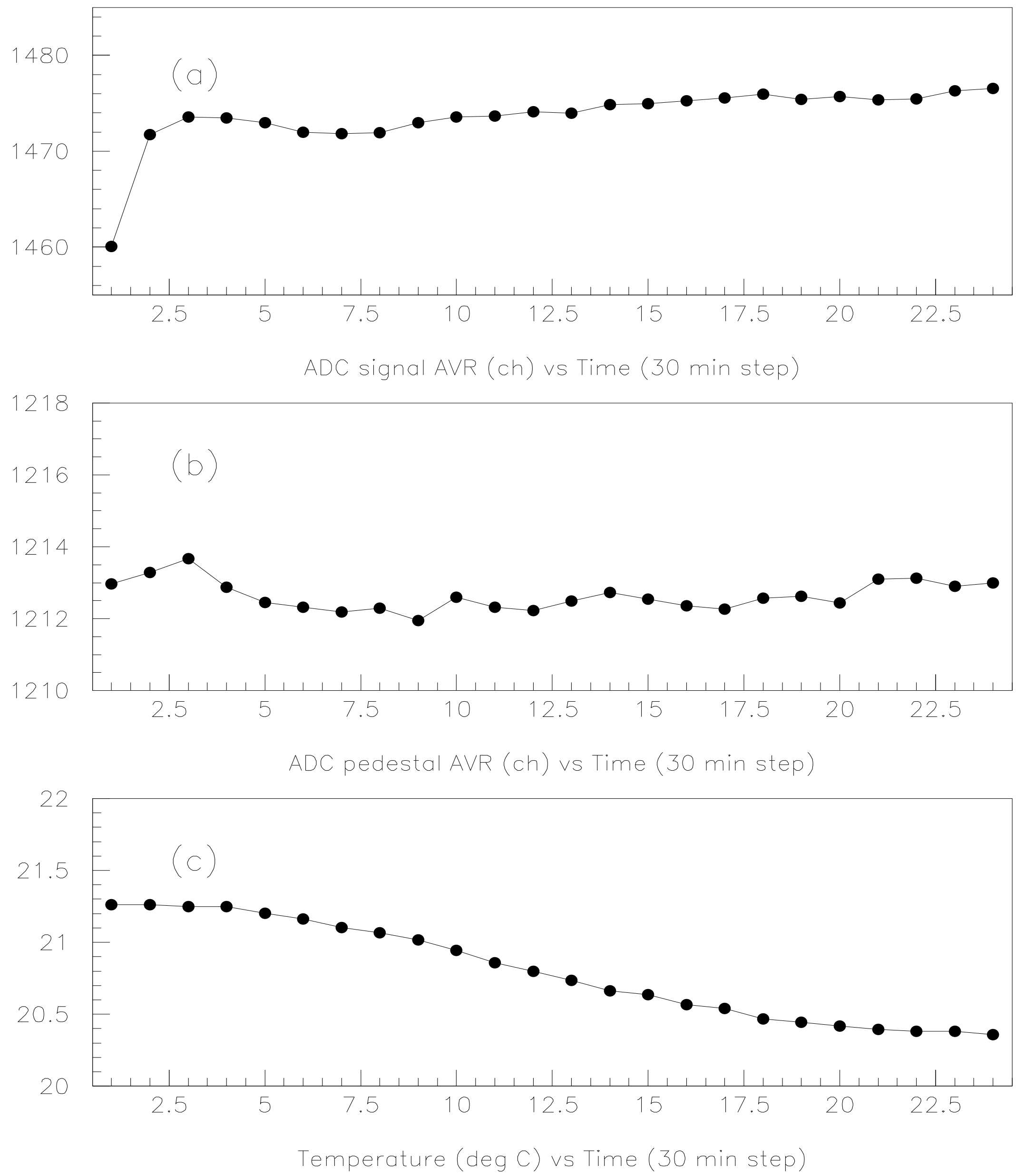

Figure 10: Variation of the centroid of the signal (a), pedestal (b) and the temperature (c) inside Photon 4 during 23 hours of monitoring. Each sample contained 5000 events. The lead-glass signal was connected to ADC channel number 14. The LED was triggered by a 30 nsec pulse of +5 V, at a repetition rate of 1 kHz. The phototube voltage was −1500 V. The ADC gate was 100 nsec. The signal increase exceeds the pedestal increase.

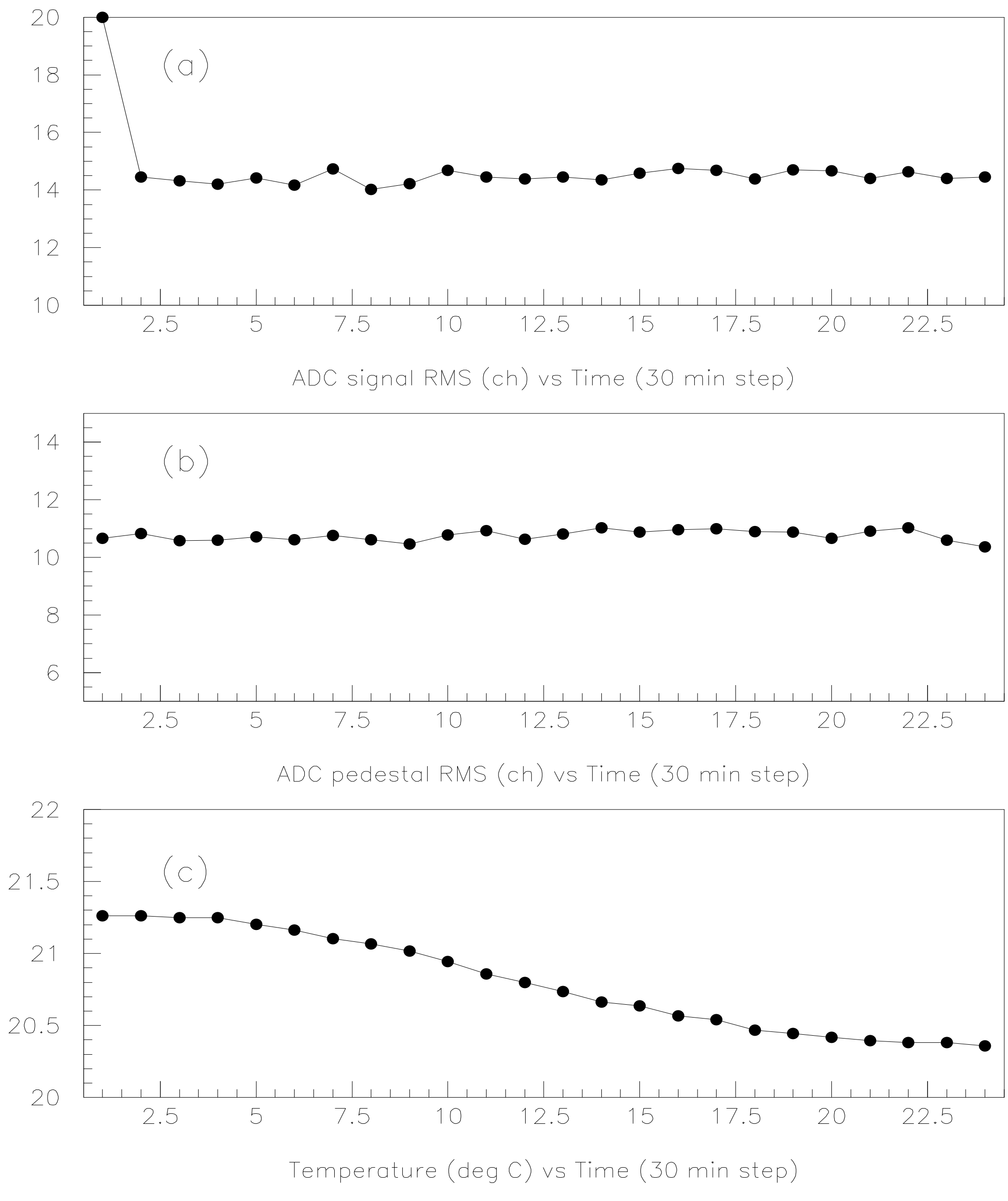

Figure 11: Variation of the rms width of the signal (a), of the pedestal(b) and the temperature (c) inside Photon 4 during 23 hours of monitoring. Each sample contained 5000 events. The lead-glass signal was connected to ADC channel number 14. The LED was triggered by a 30 nsec pulse of +5 V, at a repetition rate of 1 kHz. The phototube voltage was −1500 V. The ADC gate was 100 nsec. The signal increase exceeds the pedestal increase, and both are larger for lower temperature.

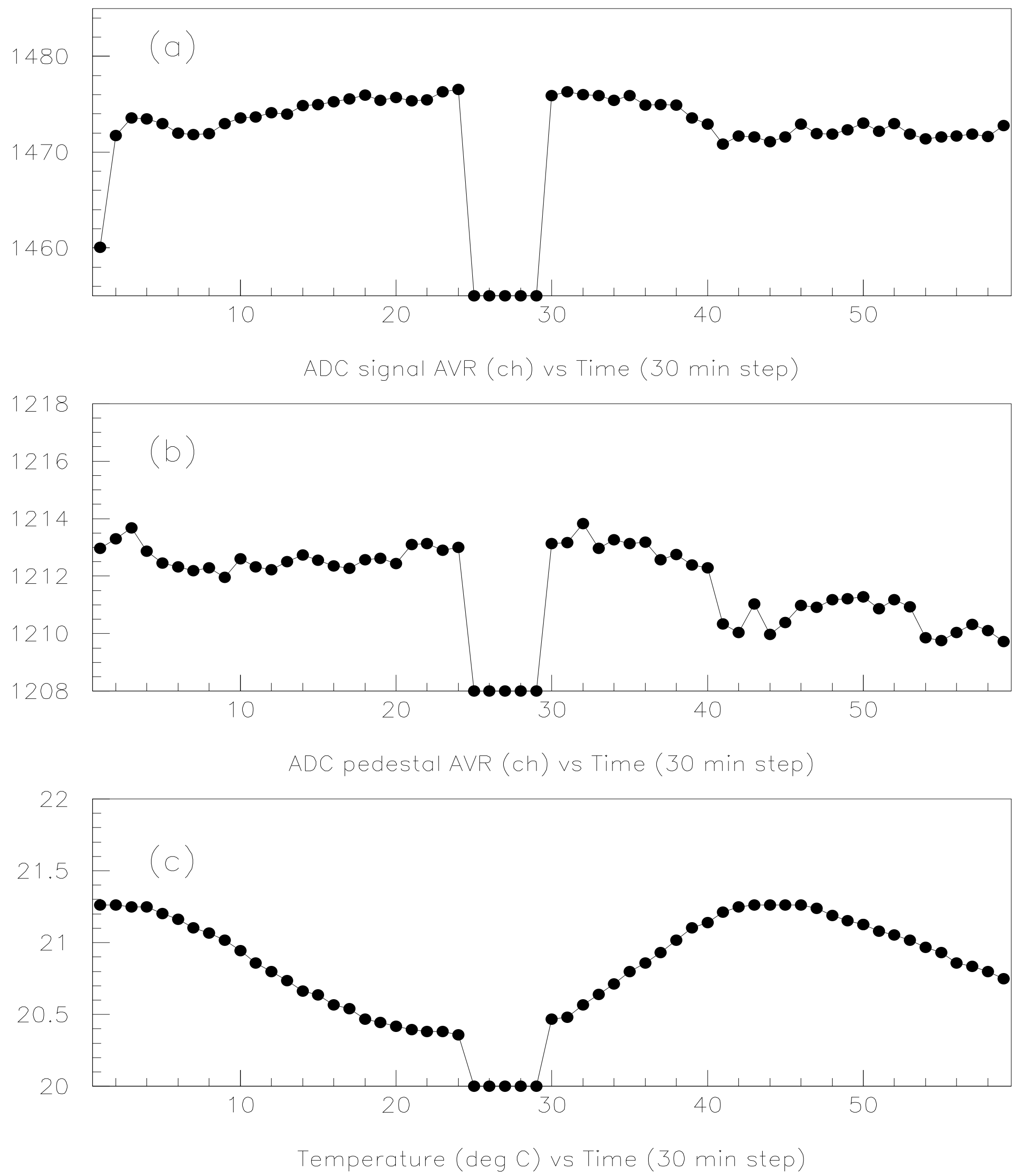

Figure 12: Variation of the centroid of the signal (a), pedestal (b) and the temperature (c) inside Photon 4 during 58 hours of monitoring. (There was a interruption of the monitoring in the middle of the period.) Each sample contained 5000 events. The lead-glass signal was connected to ADC channel number 14. The LED was triggered by a 30 nsec pulse of +5 V, at a repetition rate of 1 kHz. The phototube voltage was -1500 V. The ADC gate was 100 nsec. The signal increase exceeds by $2-3$ channels the pedestal increase, and both are larger for lower temperature.

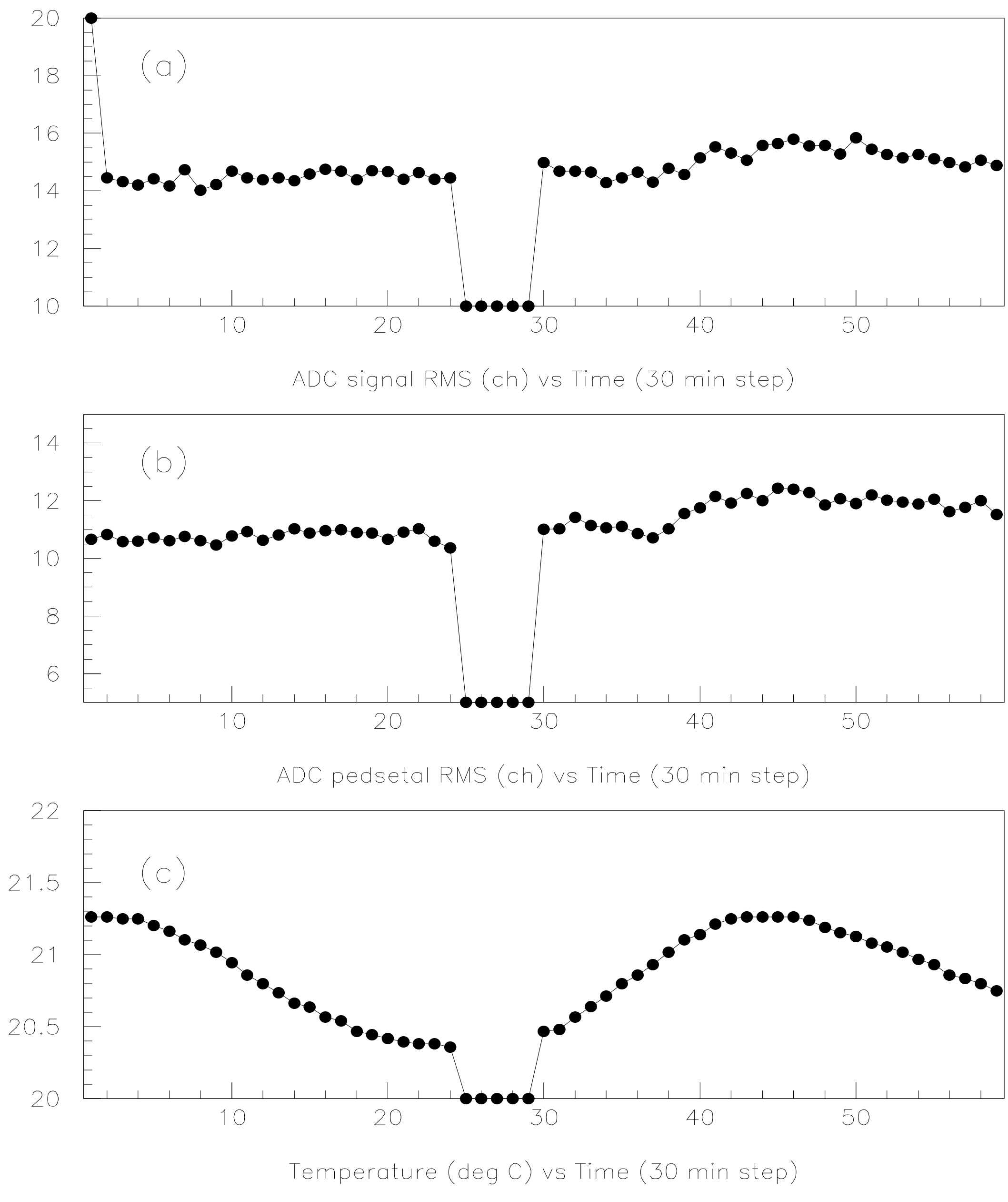

Figure 13: Variation of the rms width for the signal (a), for the pedestal(b) and the temperature (c) inside Photon 4 during 60 hours of monitoring. (There was a interruption in the middle of the period.) Each sample contained 5000 events. The lead-glass signal was connected to ADC channel number 14. The LED was triggered by a 30 nsec pulse of +5 V, at a repetition rate of 1 kHz. The phototube voltage was −1500 V. The ADC gate was 100 nsec. The widths of both signal and pedestal seem to increase at larger temperature.

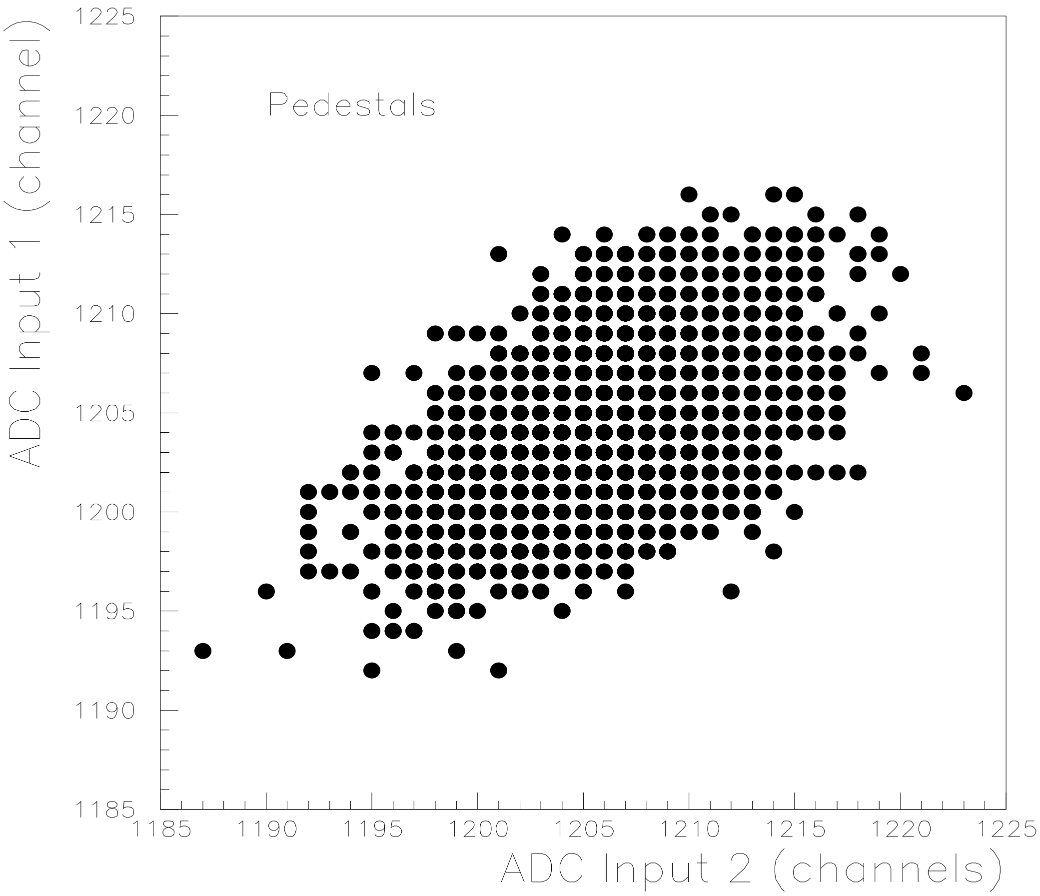

Figure 14: Pulse-to-pulse correlation of 5000 pedestals taken simultaneously in two neighboring ADC channels. This correlation may be due to the slow 60 Hz mode and its harmonics in the cables. More recent work on grounding the system has reduced the pedestal noise (see the text for more explainations).

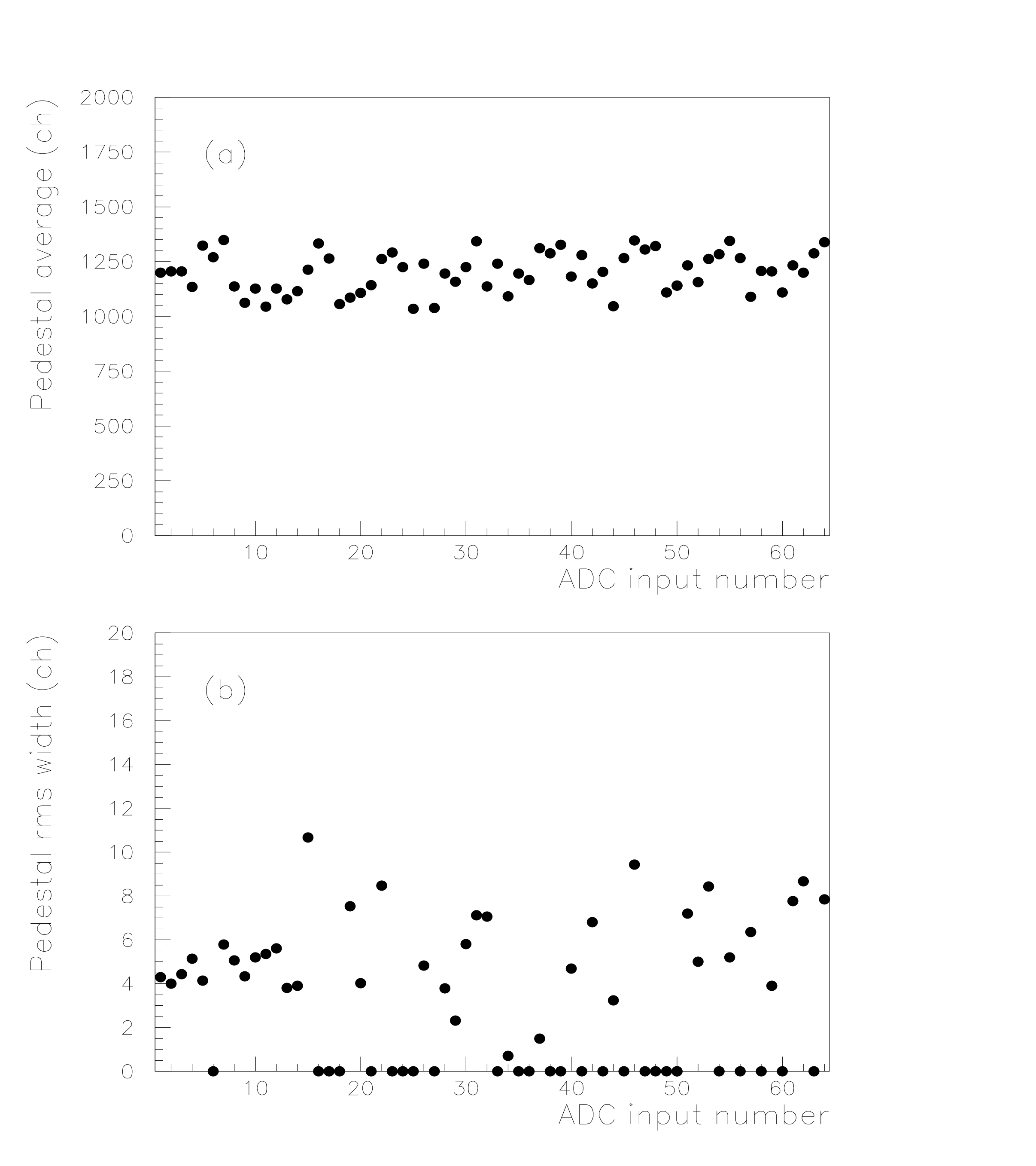

Figure 15: Average pedestal (a) and its rms width (b) as a function of the ADC input number. Each point is derived form a sample of 5000 events. The LED was triggered by a 30 nsec pulse of +5 V at a repetition rate of 1 kHz. The phototube voltage was −1500 V. The ADC gate was 100 nsec. More recent work on grounding the system has reduced the rms width of the pedestals (see the text for more explainations).

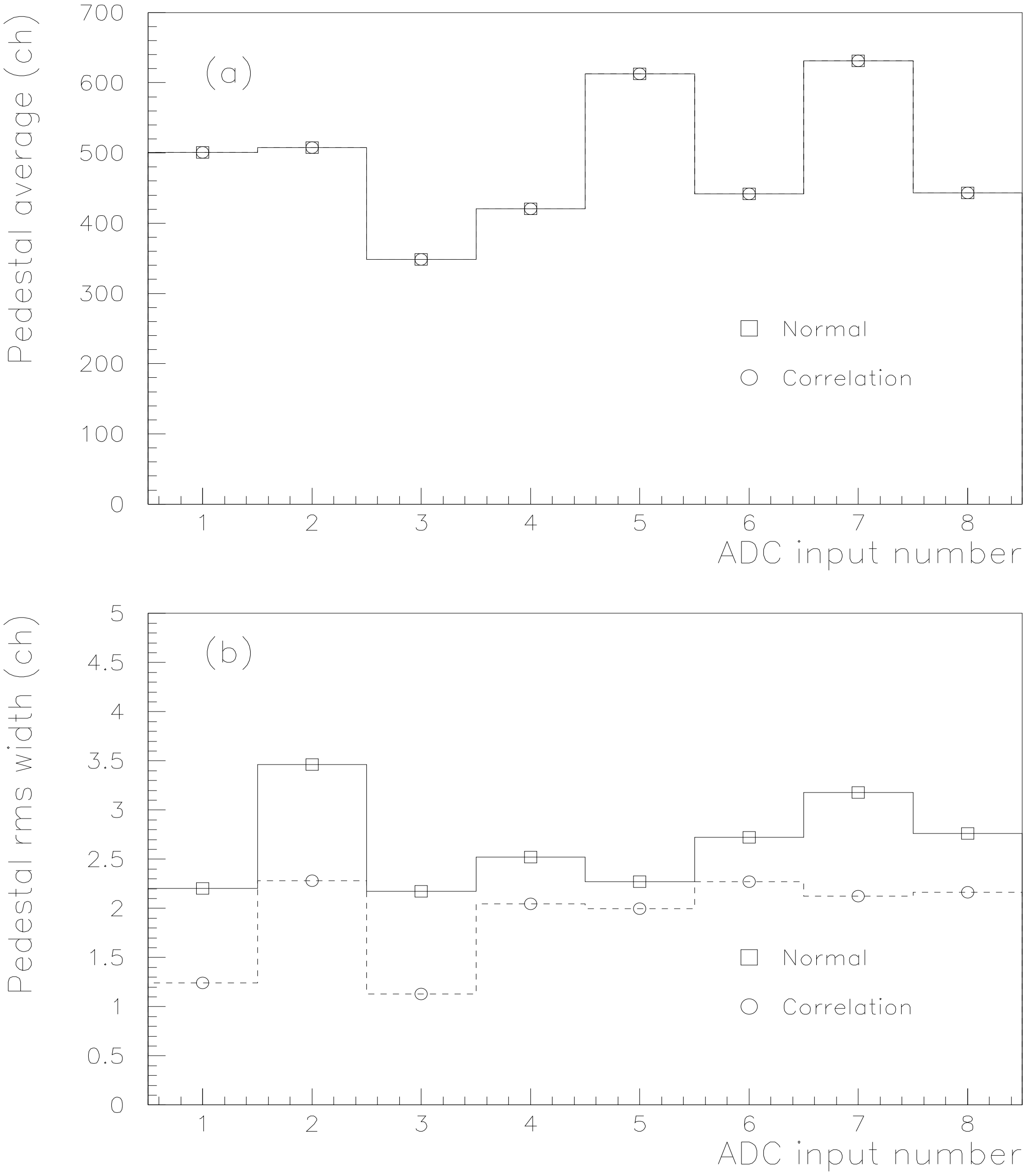

Figure 16: Average pedestal (a) and its rms width (b) for ADC input numbers $1-8$. This measurement was done during September-December 1994 tests. The open squares reprezent a normal measurement, while the open circles correspond to a measurement in which seven ADC inputs were correlated to the eighth.

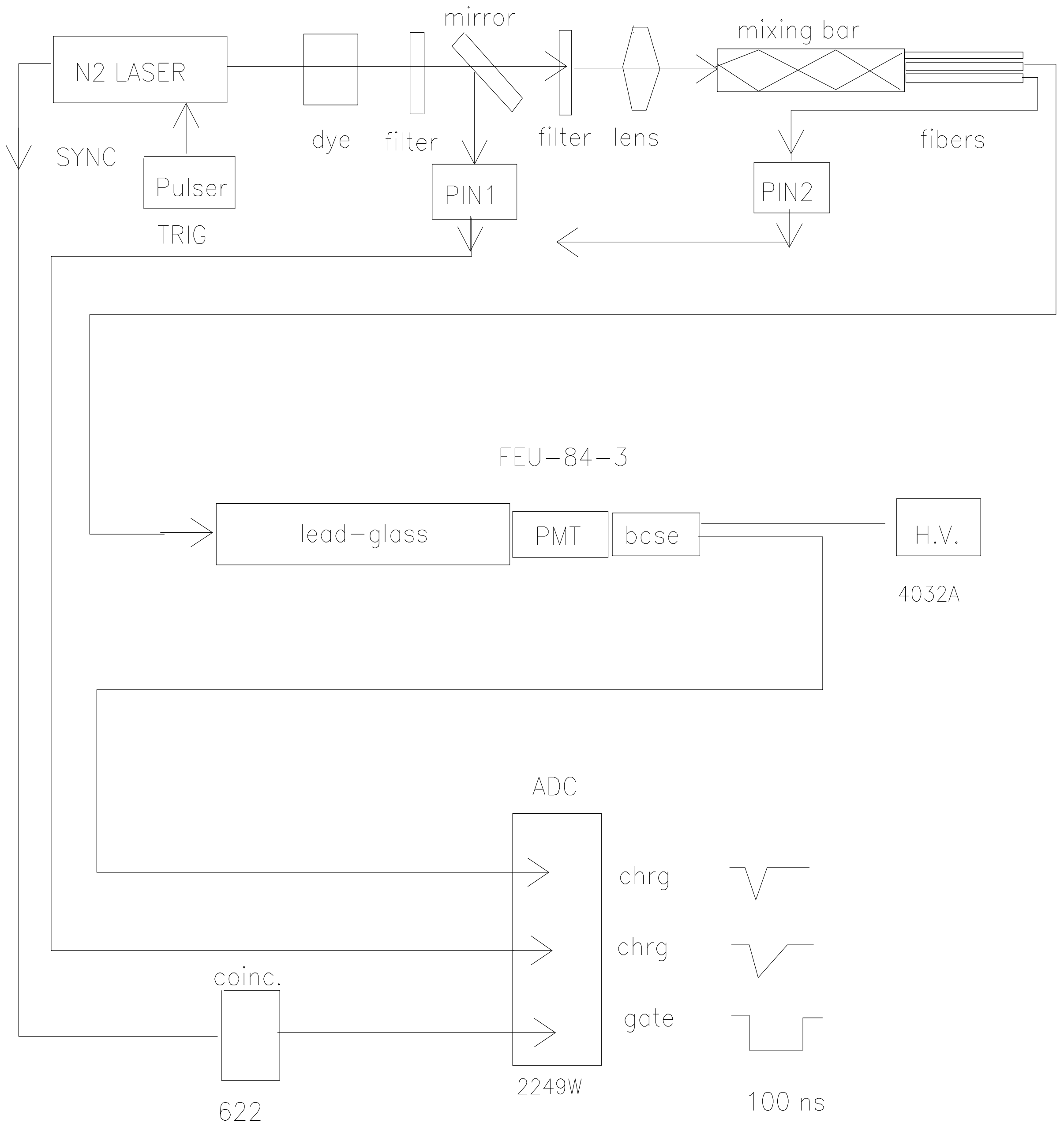

Figure 17: Basic experimental setup used during lead-glass tests at Tel-Aviv Univ.

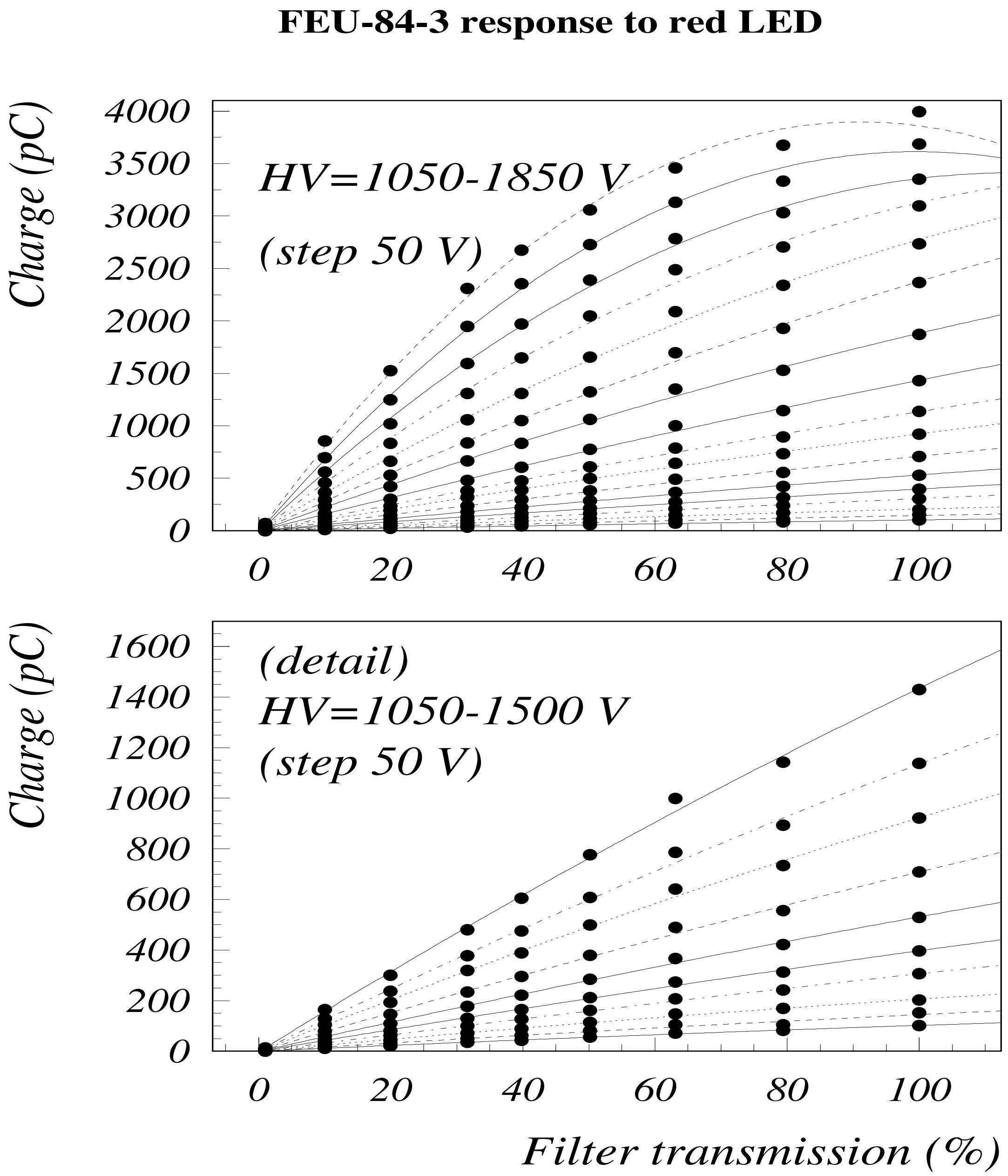

Figure 18: Response of the lead-glass to a red LED with an equivalent energy of 12 GeV for several light attenuations and for high voltages between $1050-1850$ V, with 50 V step.

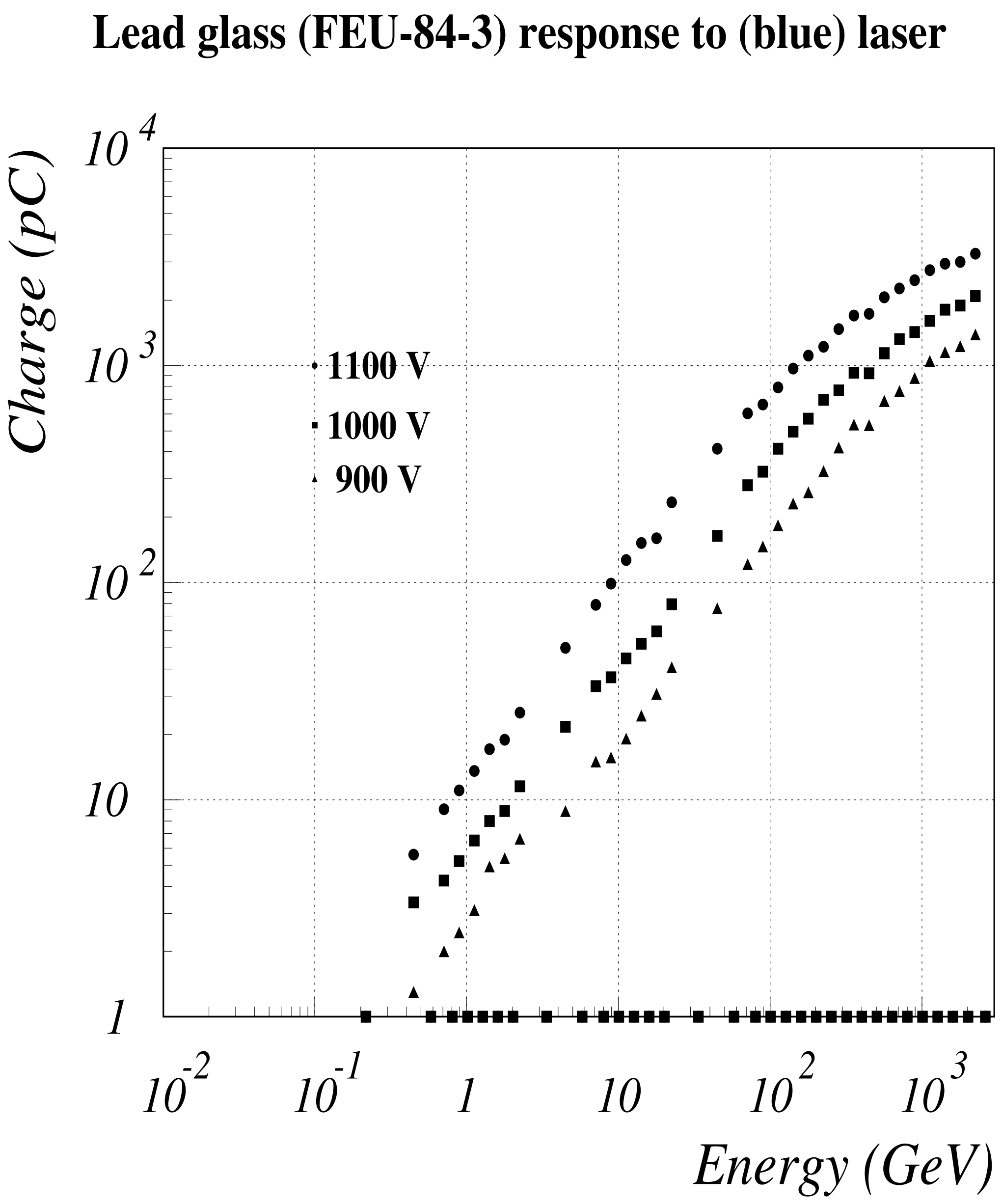

Figure 19: Response of the lead-glass to laser light with an equivalent energy of 500 GeV for several light attenuations and phototube high voltages